

Titre: Development of a 3D analytical solution to evaluate stresses in backfilled vertical openings
Title:

Auteurs: Li Li, Michel Aubertin, & Tikou Belem
Authors:

Date: 2005

Type: Rapport / Report

Référence: Li, L., Aubertin, M., & Belem, T. (2005). Development of a 3D analytical solution to evaluate stresses in backfilled vertical openings. (Rapport technique n° EPM-RT-2005-04). <https://publications.polymtl.ca/3142/>
Citation:

 **Document en libre accès dans PolyPublie**
Open Access document in PolyPublie

URL de PolyPublie: <https://publications.polymtl.ca/3142/>
PolyPublie URL:

Version: Version officielle de l'éditeur / Published version

Conditions d'utilisation: Tous droits réservés / All rights reserved
Terms of Use:

 **Document publié chez l'éditeur officiel**
Document issued by the official publisher

Institution: École Polytechnique de Montréal

Numéro de rapport: EPM-RT-2005-04
Report number:

URL officiel:
Official URL:

Mention légale:
Legal notice:

EPM-RT-2005-04

**DEVELOPMENT OF A 3D ANALYTICAL SOLUTION TO
EVALUATE STRESSES IN BACKFILLED VERTICAL
OPENINGS**

Li Li, Michel Aubertin, Tikou Belem
Département des Génies civil, géologique et des mines
École Polytechnique de Montréal

Avril 2005

Poly

EPM-RT-2005-04

**DEVELOPMENT OF A 3D ANALYTICAL SOLUTION TO EVALUATE
STRESSES IN BACKFILLED VERTICAL OPENINGS**

Li LI¹, Michel AUBERTIN^{1,3}, Tikou BELEM²

¹Department of Civil, Geological and Mining Engineering, École Polytechnique de Montréal,
C.P. 6079, Succursale Centre-ville, Québec, H3C 3A7, Canada

²Department of Applied Sciences, Université du Québec en Abitibi-Témiscamingue
445 boulevard de l'Université, Rouyn-Noranda, Québec, J9X 5E4, Canada

³Industrial NSERC Polytechnique-UQAT Chair on Environment and Mine Wastes Management
(<http://www.polymtl.ca/enviro-geremi/>).

AVRIL 2005

©2005
Li Li, Michel Aubertin, Tikou Belem
Tous droits réservés

Dépôt légal :
Bibliothèque nationale du Québec, 2005
Bibliothèque nationale du Canada, 2005

EPM-RT-2005-04

Development of a 3D analytical solution to evaluate stresses in backfilled vertical openings

par : Li Li¹, Michel Aubertin^{2,3}, Tikou Belem²

¹Department of Civil, Geological and Mining Engineering, École Polytechnique de Montréal

²Department of Applied Sciences, Université du Québec en Abitibi-Témiscamingue

³Industrial NSERC Polytechnique-UQAT Chair on Environment and Mine Wastes Management

Toute reproduction de ce document à des fins d'étude personnelle ou de recherche est autorisée à la condition que la citation ci-dessus y soit mentionnée.

Tout autre usage doit faire l'objet d'une autorisation écrite des auteurs. Les demandes peuvent être adressées directement aux auteurs (consulter le bottin sur le site <http://www.polymtl.ca/>) ou par l'entremise de la Bibliothèque :

École Polytechnique de Montréal
Bibliothèque – Service de fourniture de documents
Case postale 6079, Succursale «Centre-Ville»
Montréal (Québec)
Canada H3C 3A7

Téléphone : (514) 340-4846
Télécopie : (514) 340-4026
Courrier électronique : biblio.sfd@courriel.polymtl.ca

Ce rapport technique peut-être repéré par auteur et par titre dans le catalogue de la Bibliothèque :
<http://www.polymtl.ca/biblio/catalogue/>

ABSTRACT

The mechanical response of backfill in narrow openings is significantly influenced by its interaction with the surrounding walls. Previous work conducted on backfilled trenches and mining stopes indicates that the theory of arching can be used to estimate earth pressures in narrow, vertical backfilled openings. In this report, a 3D analytical solution is proposed to evaluate the state of stress along the boundaries of the openings. The proposed solution, based on a generalized version of the Marston approach, is compared to numerical modeling and laboratory experimental results taken from the literature. A discussion follows on some particular features and limitations of the analytical solutions.

Key words: backfill, earth pressure, 3D openings, analytical solutions, trenches, mining stopes.

RÉSUMÉ

La réponse mécanique du remblai placé dans des ouvertures étroites est largement influencée par son interaction avec les parois adjacentes. Les travaux antérieurs portant sur les tranchées et les chantiers remblayés montrent que la théorie de l'effet d'arche peut être utilisée pour estimer la pression dans les ouvertures étroites. Dans cet article, une solution analytique tridimensionnelle est proposée pour évaluer l'état de contraintes dans le remblai le long des parois de l'ouverture. La solution, basée sur une généralisation de l'approche de Marston, est comparée avec des résultats numériques et expérimentaux de laboratoire tirés de la littérature. L'article se termine par une discussion sur certaines caractéristiques et limitations de la solution analytique.

Mots clés: remblai, pression, ouvertures 3D, solutions analytiques, tranchées, chantiers miniers.

TABLE OF CONTENTS

ABSTRACT	ii
RÉSUMÉ	ii
TABLE OF CONTENTS	iii
LIST OF TABLES	iv
LIST OF FIGURES	v
LIST OF SYMBOLS	vii
1. INTRODUCTION	1
1.1 Arching concept and solutions	2
2. PROPOSED 3D ANALYTICAL SOLUTIONS	3
2.1 Theoretical development	3
2.2 Special cases	9
2.3 Graphical representation	10
3. COMPARISON WITH NUMERICAL MODELING RESULTS	15
4. APPLICATION TO LABORATORY DATA	18
5. EXTENSION TO CYLINDRICAL BINS	21
6. DISCUSSION	25
7. CONCLUSION	27
ACKNOWLEDGEMENT	28
REFERENCES	28

LIST OF TABLES

- Table 1.** Definition of K_i and α_i (in eq. [11]) for different pressure fill conditions.
- Table 2.** Internal (ϕ) and interface (δ) friction angles for the backfill (after Take and Valsangkar 2001).
- Table 3.** Parameters used in the calculation results presented in Figs. 11 – 13, base on data taken from Take and Valsangkar (2001).
- Table 4.** Parameters used in the calculation results presented in Figs. 14 – 16, base on data taken from Blight (1986*a, b*).

LIST OF FIGURES

- Fig. 1.** A vertical backfilled opening with acting forces on an isolated layer element.
- Fig. 2.** Calculated values of vertical (a), horizontal (b), and shear (c) stresses versus elevation h ; $B = 5$ m, $L = 10$ m, $c_1 = c_2 = c_3 = c_4 = c = 1$ kPa, $\phi = 35^\circ$, $\gamma = 0.02$ MN/m³; the fill is at rest ($K_1 = K_2 = K_3 = K_4 = K = 1 - \sin\phi$ and $\alpha_1 = \alpha_2 = \alpha_3 = \alpha_4 = \alpha = 0$); three cases are concerned: a base case ($\delta_1 = 10^\circ$, $\delta_2 = 20^\circ$, $\delta_3 = 30^\circ$, $\delta_4 = 35^\circ$), the upper bound limit ($\delta_1 = \delta_2 = \delta_3 = \delta_4 = 10^\circ$) and the lower bound limit ($\delta_1 = \delta_2 = \delta_3 = \delta_4 = 35^\circ$).
- Fig. 3.** Calculated values of vertical (a), horizontal (b), and shear (c) stresses versus elevation h ; $B = 5$ m, $L = 10$ m, $c_1 = c_2 = c_3 = c_4 = c = 1$ kPa, $\phi = 35^\circ$, $\gamma = 0.02$ MN/m³; the fill is in active state ($K_1 = K_2 = K_3 = K_4 = K$, $\alpha_1 = \alpha_2 = \alpha_3 = \alpha_4 = \alpha$; see Table 1); base case ($\delta_1 = 10^\circ$, $\delta_2 = 20^\circ$, $\delta_3 = 30^\circ$, $\delta_4 = 35^\circ$), upper bound limit ($\delta_1 = \delta_2 = \delta_3 = \delta_4 = 10^\circ$) and lower bound limit ($\delta_1 = \delta_2 = \delta_3 = \delta_4 = 35^\circ$).
- Fig. 4.** Calculated values of vertical (a), horizontal (b), and shear (c) stresses versus elevation h ; $B = 5$ m, $L = 10$ m, $c_1 = c_2 = c_3 = c_4 = c = 1$ kPa, $\phi = 35^\circ$, $\gamma = 0.02$ MN/m³; the fill is in passive state ($K_1 = K_2 = K_3 = K_4 = K$, $\alpha_1 = \alpha_2 = \alpha_3 = \alpha_4 = \alpha$; see Table 1); base case ($\delta_1 = 10^\circ$, $\delta_2 = 20^\circ$, $\delta_3 = 30^\circ$, $\delta_4 = 35^\circ$), the upper bound limit ($\delta_1 = \delta_2 = \delta_3 = \delta_4 = 10^\circ$) and the lower bound limit ($\delta_1 = \delta_2 = \delta_3 = \delta_4 = 35^\circ$).
- Fig. 5.** Calculated values of vertical (a), horizontal (b), transverse (c), and longitudinal shear (d) stresses versus elevation h ; $B = 5$ m, $L = 10$ m, $\phi = 35^\circ$, $\gamma = 0.02$ MN/m³, $\delta_1 = 10^\circ$, $\delta_2 = 20^\circ$, $\delta_3 = 30^\circ$, and $\delta_4 = 35^\circ$; the fill is in at rest state (see Table 1).
- Fig. 6.** Calculated values of vertical (a), horizontal (b) stresses versus the ratio h/B obtained using 2D (eq. [30]) and 3D (eq. [29]) solutions with the fill in at rest state (see Table 1); $B = 6$ m, $L = 10$ m, $c = 0.001$ MPa, $\delta = \phi = 30^\circ$, $K = 1 - \sin\phi = 0.5$, $\gamma = 0.02$ MN/m³.
- Fig. 7.** Calculated values of vertical (a), horizontal (b) stresses versus length to width ratio L/B obtained using the 2D (eq. [30]) and 3D (eq. [29]) solutions with the fill in at rest state (see Table 1); $B = 6$ m, $h = 10$ m, $c = 0.001$ MPa, $\delta = \phi = 30^\circ$, $\gamma = 0.02$ MN/m³.

- Fig. 8.** Numerical model geometry of a narrow backfilled stope (not to scale) for FLAC-2D (Itasca 2002); the main properties for the rock mass and backfill are given using classical geomechanical notations.
- Fig. 9.** Comparison of vertical (a), and horizontal (b) stresses along the vertical central line (VCL) and left wall (LW) obtained from the numerical modeling and the analytical solutions, with $c_1 = c_3 = c = 0$ kPa, $\delta_1 = \delta_3 = \phi = 35^\circ$.
- Fig. 10.** Comparison between the numerical model and the analytical solutions for vertical (a), horizontal (b) and shear (c) stresses versus the opening height, with $c_1 = c_3 = c = 0$ kPa, $\delta_1 = 25^\circ$, $\delta_3 = \phi = 35^\circ$.
- Fig. 11.** Comparison between the proposed solution (eqs. [19] and [29]) and experimental results obtained on 3D physical model backfilled with dense sand (data taken from Take and Valsangkar 2001; see text for details).
- Fig. 12.** Comparison between the proposed general solution (eq. [18] and [19]) and the experimental results obtained on a 3D physical model backfilled with dense sand (data taken from Take and Valsangkar 2001; see text for details).
- Fig. 13.** Comparison between the proposed solution (eqs. [18] and [19]) and experimental results obtained on a 3D physical model backfilled with loose sand (data taken from Take and Valsangkar 2001; see text for details).
- Fig. 14.** Comparison between the proposed solution (eq. [38]) and the experimental measurements made in coal load-out silo; $D = 20$ m (data taken from Fig. 6 in Blight 1986a).
- Fig. 15.** Comparison between the proposed solution (eq. [38]) and the experimental measurements made in a grain silo; $D = 7$ m (data taken from Fig. 9 in Blight 1986a).
- Fig. 16.** Comparison between the proposed solution (eq. [38]) and the experimental measurements made in a fine powder silo; $D = 15$ m (data taken from Fig. 5 in Blight 1986b).

LIST OF SYMBOLS

A , cross section area of an opening;

B , opening width;

BW, back wall of an opening;

c , fill cohesion;

c_i , cohesion of the i^{th} fill-wall interface ($i = 1$ to 4);

C_i , lateral compressive forces on the i^{th} wall ($i = 1$ to 4);

D , diameter of a silo;

dh , thickness of layer element;

FW, front wall of an opening;

g , the gravity acceleration;

h , elevation in backfill;

H , backfill height;

K_i , reaction coefficient for cohesionless material on the i^{th} wall ($i = 1$ to 4);

K_0 , at rest reaction coefficient for cohesionless material;

K_a , active reaction coefficient for cohesionless material;

K_{ci} , coefficient of lateral pressure ($i = 1$ to 4) for cohesive or cohesionless fill material;

K_p , passive reaction coefficient for cohesionless material;

L , opening length;

LW, left wall of an opening;

P , cross section perimeter of an opening;

RW, right wall of an opening;

S_B (and $S_B + dS_B$), backfill material transverse internal shearing force;

S_i , vertical fill-wall shearing force on the i^{th} wall ($i = 1$ to 4);

S_L (and $S_L + dS_L$), backfill material longitudinal internal shearing force;

T_i , horizontal fill-wall shearing force on the i^{th} wall ($i = 1$ to 4);

V (and $V + dV$), internal vertical force;

VCL, vertical central line;

W , weight of the backfill;

z , depth of a modeled slope;

α_i , backfill state angle on the i^{th} wall ($i = 1$ to 4);

δ , a unique value of wall-fill friction angle;

δ_i , the friction angle of the i^{th} fill-wall interface ($i = 1$ to 4);

ϕ , fill friction angle;

γ , unit weight of backfill;

κ_{13} and κ_{24} , parameters defined in eq. [16];

λ_{13} and λ_{24} , parameters defined in eq. [17];

ν , Poisson ratio;

σ_{hi} , horizontal stress on the i^{th} wall ($i = 1$ to 4);

σ_{vh} , vertical stress at position h ;

τ_B , transverse shear stress;

τ_L , longitudinal shear stress.

1. INTRODUCTION

Many situations encountered in geotechnique require a quantitative evaluation of the loading conditions induced by backfill placed in confined narrow openings. Examples include load on conduits in trenches (e.g., Spangler and Handy 1984; McCarthy 1988), lateral stress on retaining walls (Frydman and Keissar 1987), vertical stress above tunnels (Iglesia et al. 1999), and pressure in backfilled mined stopes (e.g., Hustrulid et al. 1989; Aubertin et al. 2003; Harvey 2004; Belem et al. 2004). The latter applications are of particular interest to the authors as the practice of stope backfilling is increasingly important in mining around the world, for reasons of ground stability (e.g., Thomas et al. 1979; Singh and Hedley 1981; Hassani and Archibald 1998; Kump 2001; Jung and Biswas 2002) and also for improved mine waste management (Aubertin et al. 2002).

The backfill material placed in openings is usually much softer than that of the surrounding walls, which are often made of concrete or rock. As backfill tends to settle under its own weight, the two types of media interact in a complex manner. The characteristics of the fill material and of the walls must therefore be taken into account to evaluate the induced stress distribution in and around the openings. Numerical modeling tools constitute powerful means to investigate the response of such systems, as they can consider various factors such as natural stress conditions, excavation and placement sequence and discontinuities (e.g., Pariseau 1981; Hustrulid et al. 1989; Brummer et al. 1996; Brechtel et al. 1999; Li et al. 2003). Nevertheless, analytical methods may also provide rapid, low cost and valuable solutions for evaluating the behavior of backfilled openings (e.g., Knutsson 1981; Mitchell 1983; Aubertin et al. 2003; Belem et al. 2004; James et al. 2004). Previous work on this issue, including some recent studies conducted by the authors, indicates that the theory of arching may be well suited for estimating the earth pressures in narrow vertical openings (e.g., Handy 1985; Aubertin 1999; Take and Valsangkar 2001; Aubertin et al. 2003; Li et al. 2003). However, most existing arching solutions are based on 2D limit equilibrium analysis, in which the two long walls of the opening are identical. In some practical cases, such solutions are incomplete, especially when the backfilled opening has a limited length or when the walls have different characteristics.

In this report, a general 3D analytical solution is proposed. Its validity is demonstrated, at least in part, using numerical modeling and representative experimental results. A discussion follows on the main assumptions and limitations of the proposed approach.

1.1 Arching concept and solutions

When a frictional particulate material is placed in a confined narrow opening, the fill tends to yield as it moves downward. The surrounding rigid walls then hold the yielding material by shear forces along the interfaces. Part of the load due to the weight of the material is thus transferred to the walls, so the resulting vertical stress in the fill is reduced. This type of phenomenon is known as arching (e.g., Richmond and Gardner 1962; Handy 1985; Hunt 1986).

Arching effects have been observed in many situations, particularly within silos and bins used to store particulate materials. Handling materials such as powder and grain requires an estimate of the minimum span needed to avoid the formation of a stable arch in the containers (e.g., Richards 1966; Cowin 1977; Blight 1986*a*, *b*). The basic arching theory, initially proposed by Janssen (1895), is often used to analyse this type of situation. Arching was later introduced to geotechnical engineering by Marston (1930) and his team, for calculating pressures on underground conduits placed in ditches (see also Handy 1985; McCarthy 1988), and by Terzaghi (1936, 1943) to evaluate the stress distribution above tunnels (e.g., Ladanyi and Hoyaux 1969; Atkinson and Cairncross 1974). Arching theory has also been applied to retaining walls (Frydman and Keissar 1987; Take and Valsangkar 2001) and to dams (Kutzner 1997).

In geotechnique, many of the above mentioned types of structure have a dimension that is much larger than the other two, so most practical problems are treated with 2D (plane strain) models (e.g., Hustrulid et al. 1989; Iglesia et al. 1999; Aubertin et al. 2003). Nevertheless, there are exceptions, including the solution given by Van Horn (1964) who used the Marston theory to obtain three dimensional loads on underground structures. Three dimensional considerations have also been given to cases where one of the retaining walls around the opening is removed (e.g., Mitchell 1983).

In the powder and grain industry on the other hand, containers have finite dimensions on all sides, so three dimensional models have typically been adopted (e.g., Richmond and Gardner 1962; Richards 1966; Cowin 1977; Blight 1986*a, b*; Williams et al. 1987); these solutions are often axisymmetric.

With most existing (2D and 3D) solutions, a unique fill-wall friction angle is used. In practice, it is not uncommon that the walls around vertical openings have different characteristics.

In the following, a set of 3D equations is developed to evaluate the stress along vertical walls of narrow backfilled openings having different properties; the proposed equations are extensions of those recently proposed by Li et al. (2004).

2. PROPOSED 3D ANALYTICAL SOLUTIONS

2.1 Theoretical development

Figure 1 shows schematically a vertical, narrow backfilled opening, with the various forces on a layer element, based on uniformly distributed stresses on the isolated layer. This representation is based on the model proposed by Marston (1930) for 2D conditions (see also Handy 1985; McCarthy 1988). In Figure 1, H is the backfill height, B is the opening width and L is its length. The four walls are identified as 1 for left wall (LW), 2 for front wall (FW), 3 for right wall (RW) and 4 for back wall (BW). At position h , the horizontal layer element is subjected to lateral compressive forces C_i ($i = 1$ to 4), vertical and horizontal fill-wall shearing forces S_i and T_i ($i = 1$ to 4), backfill material longitudinal and transverse internal shearing forces S_L (and $S_L + dS_L$) and S_B (and $S_B + dS_B$), and internal vertical forces V (and $V + dV$). Based on this representation, general 3D equations can be developed, as described below.

The weight of the backfill W in the thin layer element is given by:

$$[1] \quad W = \gamma B L dh$$

where γ is the unit weight of the backfill, and dh is the thickness of the layer element.

The vertical force V is obtained by assuming a uniform vertical stress distribution along the horizontal plane (this and other assumptions will be discussed later in the report). The vertical force can then be expressed as:

[2]

$$V = \sigma_{vh} B L$$

where σ_{vh} is the vertical stress at position h .

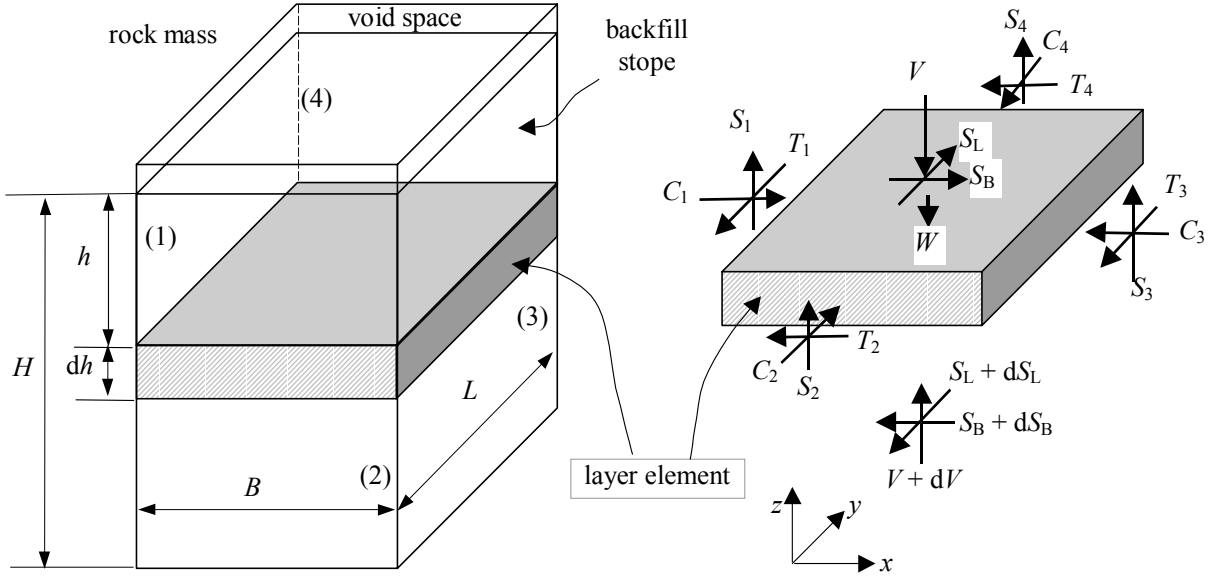


Fig. 1. A vertical backfilled opening with acting forces on an isolated layer element.

The longitudinal (S_L) and transverse (S_B) shearing forces are expressed as:

$$[3a] \quad S_L = \tau_L B L$$

$$[3b] \quad S_B = \tau_B B L$$

where τ_L and τ_B are the longitudinal and transverse shear stresses, respectively. These are also assumed to be uniformly distributed on the horizontal plane.

Using a linear relationship between the vertical stress σ_{vh} and horizontal stress σ_{hhi} ($i = 1$ to 4) in the backfill layer element, the lateral compressive force C_i ($i = 1$ to 4) on each wall can be expressed as:

$$[4a] \quad C_j = dh L \sigma_{hij} = dh L K_{cj} \sigma_{vh} = dh K_{cj} V/B, \text{ for } j = 1, 3$$

$$[4b] \quad C_k = dh B \sigma_{hik} = dh B K_{ck} \sigma_{vh} = dh K_{ck} V/L, \text{ for } k = 2, 4$$

where the coefficient of lateral pressure K_{ci} ($i = j, k$) is the ratio of the horizontal stress to vertical stress at the i^{th} fill-wall interface:

$$[5] \quad K_{ci} = \sigma_{hi}/\sigma_{vh}$$

For conditions where the walls do not move and the lateral strain is zero (the “at rest” condition), the coefficient of lateral pressure can be empirically defined as (Jaky 1948):

$$[6] \quad K_{ci} = K_{0i} = 1 - \sin\phi$$

The value of K_{0i} could also be defined using an elastic solution, as a function of Poisson ratio ν (Jaeger and Cook 1979). For typical values of ϕ and ν , the values of K_{0i} obtained by both approaches are often very similar.

In some cases, the wall may move outward, away from the opening, due to the backfill pressure. In such a case, the coefficient K_{ci} is sometimes approximated by the Rankine active earth pressure coefficient (see discussion below). The reaction coefficient is then expressed as:

$$[7] \quad K_{ci} = K_{ai} - \frac{2c}{\sigma_{vh}} \tan\left(45^\circ - \frac{\phi}{2}\right)$$

where

$$[8] \quad K_{ai} = \frac{1 - \sin\phi}{1 + \sin\phi}$$

For *in situ* cases where the fill is placed between walls already under elastic equilibrium, the reaction coefficient can be expected to be somewhere between K_{0i} and K_{ai} .

Similarly, for a wall that moves inside the opening (due to convergence), K_{ci} can be taken (as a first approximation) as the Rankine passive pressure, which can be expressed as:

$$[9] \quad K_{ci} = K_{pi} + \frac{2c}{\sigma_{vh}} \tan\left(45^\circ + \frac{\phi}{2}\right)$$

where

$$[10] \quad K_{pi} = \frac{1 + \sin\phi}{1 - \sin\phi}$$

In these equations, ϕ and c are the friction angle and cohesion of the fill material, respectively.

Eqs [6], [7] and [9] can be rewritten in a unified format, as:

$$[11] \quad K_{ci} = K_i + \frac{2c}{\sigma_{vh}} \tan\alpha_i$$

The values for K_i and α_i in eq. [11] are given in Table 1; c in eq. [11] and ϕ in Table 1 are cohesion and friction angle of the fill material, respectively. For typical backfill problems with almost fixed walls, the actual value of K_i is expected to be between the at rest (K_0) and active (K_a) states, depending on the position in the opening, as was described by Frydman and Keissar (1987). Hence, calculations shown below will include both values of the coefficient of lateral pressure.

Table 1. Definition of K_i and α_i (in eq. [11]) for different fill pressure conditions.

Fill condition	K_i	α_i
At rest (K_0)	$1 - \sin\phi$	0°
Active (K_a)	$\frac{1 - \sin\phi}{1 + \sin\phi}$	$\frac{\phi}{2} - 45^\circ$
Passive (K_p)	$\frac{1 + \sin\phi}{1 - \sin\phi}$	$45^\circ + \frac{\phi}{2}$

The Coulomb criterion is used to define the shearing forces S_i ($i = 1$ to 4) along the walls:

$$[12a] \quad S_j = (\sigma_{nhj} \tan\delta_j + c_j) L dh = (K_{cj} \sigma_{vh} \tan\delta_j + c_j) L dh, \text{ for } j = 1, 3$$

$$[12b] \quad S_k = (\sigma_{hkh} \tan\delta_k + c_k) B dh = (K_{ck} \sigma_{vh} \tan\delta_k + c_k) B dh, \text{ for } k = 2, 4$$

where δ_i and c_i ($i = j, k$) are the friction angle and cohesion of the i^{th} fill-wall interface, respectively.

Static equilibrium of the layer element in the vertical (z) direction implies that:

$$[13] \quad W = dV + \sum_{i=1}^4 S_i$$

Introducing eqs. [1], [2] and [12] into eq. [13] gives the following:

$$[14] \quad \frac{d\sigma_{vh}}{dh} + \sigma_{vh} \left(\frac{K_{c1} \tan \delta_1 + K_{c3} \tan \delta_3}{B} + \frac{K_{c2} \tan \delta_2 + K_{c4} \tan \delta_4}{L} \right) + \left(\frac{c_1 + c_3}{B} + \frac{c_2 + c_4}{L} \right) - \gamma = 0$$

Combining eqs. [11] and eq. [14], one then obtains:

$$[15] \quad \frac{d\sigma_{vh}}{dh} + \sigma_{vh} \left(\frac{\lambda_{13}}{B} + \frac{\lambda_{24}}{L} \right) + \left(\frac{\kappa_{13}}{B} + \frac{\kappa_{24}}{L} \right) - \gamma = 0$$

where

$$[16] \quad \begin{aligned} \lambda_{13} &= K_1 \tan \delta_1 + K_3 \tan \delta_3 \\ \lambda_{24} &= K_2 \tan \delta_2 + K_4 \tan \delta_4 \end{aligned}$$

and

$$[17] \quad \begin{aligned} \kappa_{13} &= c_1 + c_3 + 2c(\tan \alpha_1 \tan \delta_1 + \tan \alpha_3 \tan \delta_3) \\ \kappa_{24} &= c_2 + c_4 + 2c(\tan \alpha_2 \tan \delta_2 + \tan \alpha_4 \tan \delta_4) \end{aligned}$$

with $\delta_i \leq \phi$ and $c_i \leq c$ ($i = 1$ to 4). Note that for $\delta_i > \phi$ and/or $c_i > c$ along the interface, yielding is expected to take place in the fill (rather than directly along the fill-wall interface), so the values of ϕ and c are taken for δ_i and c_i , respectively.

From eq. [15], the vertical stress acting across the horizontal plane at position h is deduced as follows:

$$[18] \quad \sigma_{vh} = \frac{\gamma - (\kappa_{13} B^{-1} + \kappa_{24} L^{-1})}{(\lambda_{13} B^{-1} + \lambda_{24} L^{-1})} \left\{ 1 - \exp\left(-h(\lambda_{13} B^{-1} + \lambda_{24} L^{-1})\right) \right\}$$

With this equation, it can be shown that the value of the vertical stress tends toward the overburden pressure (γh) when the size of the opening (B, L) is large enough (i.e. when arching effects become negligible).

The horizontal stress σ_{hhi} can now be obtained from eqs. [5], [11] and [18]:

$$[19] \quad \sigma_{hhi} = K_i \sigma_{vh} + 2c \tan \alpha_i$$

On the other hand, by considering the moment equilibrium around axes x and y , one obtains:

$$[20a] \quad (S_2 - S_4) L + (2S_L + dS_L) dh = 0$$

$$[20b] \quad (S_1 - S_3) B + (2S_B + dS_B) dh = 0$$

By neglecting the second order terms ($dS_B dh$ and $dS_L dh$) which are very small, eqs. [20a, b] give:

$$[21a] \quad S_L = L (S_4 - S_2)/(2dh)$$

$$[21b] \quad S_B = B (S_3 - S_1)/(2dh)$$

Introducing eqs. [3] and [12] into these last two equations, the longitudinal (τ_L) and transverse (τ_B) shear stresses can be deduced as:

$$[22a] \quad \tau_L = \frac{K_{c4} \tan \delta_4 - K_{c2} \tan \delta_2}{2} \sigma_{vh} + \frac{c_4 - c_2}{2}$$

$$[22b] \quad \tau_B = \frac{K_{c3} \tan \delta_3 - K_{c1} \tan \delta_1}{2} \sigma_{vh} + \frac{c_3 - c_1}{2}$$

Replacing K_{ci} of eqs. [22a, b] by eq. [11], one obtains:

$$[23a] \quad \tau_L = \frac{K_4 \tan \delta_4 - K_2 \tan \delta_2}{2} \sigma_{vh} + \frac{c_4 - c_2 + 2c(\tan \alpha_4 \tan \delta_4 - \tan \alpha_2 \tan \delta_2)}{2}$$

$$[23b] \quad \tau_B = \frac{K_3 \tan \delta_3 - K_1 \tan \delta_1}{2} \sigma_{vh} + \frac{c_3 - c_1 + 2c(\tan \alpha_3 \tan \delta_3 - \tan \alpha_1 \tan \delta_1)}{2}$$

In general, the two opposite walls react in the same manner so that $K_1 = K_3$, $K_2 = K_4$, $\alpha_1 = \alpha_3$ and $\alpha_2 = \alpha_4$. In this case, eqs. [16] and [17] become:

$$[24a] \quad \begin{aligned} \lambda_{13} &= K_1 (\tan \delta_1 + \tan \delta_3) \\ \lambda_{24} &= K_2 (\tan \delta_2 + \tan \delta_4) \end{aligned}$$

$$[24b] \quad \begin{aligned} \kappa_{13} &= c_1 + c_3 + 2c(\tan \delta_1 + \tan \delta_3) \tan \alpha_1 \\ \kappa_{24} &= c_2 + c_4 + 2c(\tan \delta_2 + \tan \delta_4) \tan \alpha_2 \end{aligned}$$

Eqs. [18], [19], [23], and [24] represent the proposed 3D general solution for the stresses in vertical backfilled openings.

2.2 Special cases

When the four fill-wall interfaces have the same cohesion c , equal to that of the backfill, the following parameters are used in eqs. [18] and [19]:

$$[25a] \quad \begin{aligned} \lambda_{13} &= K_1(\tan\delta_1 + \tan\delta_3) \\ \lambda_{24} &= K_2(\tan\delta_2 + \tan\delta_4) \end{aligned}$$

$$[25b] \quad \begin{aligned} \kappa_{13} &= 2c(1 + (\tan\delta_1 + \tan\delta_3)\tan\alpha_1) \\ \kappa_{24} &= 2c(1 + (\tan\delta_2 + \tan\delta_4)\tan\alpha_2) \end{aligned}$$

Eq. [23] can then be rewritten as:

$$[26a] \quad \tau_L = (\tan\delta_4 - \tan\delta_2) \left(\frac{K_2 \sigma_{vh}}{2} + c \tan\alpha_2 \right)$$

$$[26b] \quad \tau_B = (\tan\delta_3 - \tan\delta_1) \left(\frac{K_1 \sigma_{vh}}{2} + c \tan\alpha_1 \right)$$

The case of opposite walls that have the same properties may be encountered in practical situation. For instance, in backfilled mine stopes, the hanging and foot walls are often made of one rock type while the two side (lateral) walls are made of another rock type (i.e., $\delta_1 = \delta_3$, $\delta_2 = \delta_4$, $c_1 = c_3$, and $c_2 = c_4$). In this particular case, eq. [18] becomes:

$$[27] \quad \sigma_{vh} = \frac{\gamma - 2((c_1 + 2c \tan\alpha_1 \tan\delta_1)B^{-1} + (c_2 + 2c \tan\alpha_2 \tan\delta_2)L^{-1})}{2(B^{-1}K_1 \tan\delta_1 + L^{-1}K_2 \tan\delta_2)} \left\{ 1 - \exp(-2h(B^{-1}K_1 \tan\delta_1 + L^{-1}K_2 \tan\delta_2)) \right\}$$

It is also possible that the four walls around the opening are composed of a single material (i.e., $\delta_1 = \delta_2 = \delta_3 = \delta_4 = \delta$ and $c_1 = c_2 = c_3 = c_4 = c$); eq. [18] then becomes:

$$[28] \quad \sigma_{vh} = \frac{\gamma - 2c((1 + 2 \tan\alpha_1 \tan\delta)B^{-1} + (1 + 2 \tan\alpha_2 \tan\delta)L^{-1})}{2(B^{-1}K_1 + L^{-1}K_2) \tan\delta} \left\{ 1 - \exp(-2h(B^{-1}K_1 + L^{-1}K_2) \tan\delta) \right\}$$

If the four walls react in the same manner, $K_1 = K_2 = K_3 = K_4 = K$, and $\alpha_1 = \alpha_2 = \alpha_3 = \alpha_4 = \alpha$, and eq. [28] becomes:

$$[29] \quad \sigma_{vh} = \frac{\gamma(B^{-1} + L^{-1})^{-1} - 2c(1 + 2\tan\alpha\tan\delta)}{2K\tan\delta} \left\{ 1 - \exp(-2hK(B^{-1} + L^{-1})\tan\delta) \right\}$$

This would be equivalent to the Van Horn's (1964) solution if the fill is in at rest state ($\alpha = 0$) or for a cohesionless material ($c = 0$).

If the opening length is significantly larger than its width (i.e. $L \gg B$), eq. [29] reduces to a 2D solution:

$$[30] \quad \sigma_{vh} = \frac{\gamma B - 2c(1 + 2\tan\alpha\tan\delta)}{2K\tan\delta} \left\{ 1 - \exp(-2KhB^{-1}\tan\delta) \right\}$$

For a friction angle of the fill equal to or smaller than the fill-wall friction angle (i.e. $\phi \leq \delta$), one can then write:

$$[31] \quad \sigma_{vh} = \frac{\gamma B - 2c(1 + 2\tan\alpha\tan\phi)}{2K\tan\phi} \left\{ 1 - \exp(-2KhB^{-1}\tan\phi) \right\}$$

For a cohesionless fill, eq. [31] reduces to one of the Marston's equations (McCarthy 1988; Aubertin et al. 2003) as:

$$[32] \quad \sigma_{vh} = \gamma B \left(\frac{1 - \exp(-2KhB^{-1}\tan\phi)}{2K\tan\phi} \right)$$

2.3 Graphical representation

Figure 2 shows the vertical (Fig. 2a), horizontal (Fig. 2b) and shear (Fig. 2c) stress variation in a backfilled opening using the general 3D solution (eqs. [18], [19] and [23]) with the fill and walls at rest ($K_1 = K_2 = K_3 = K_4 = K = 1 - \sin\phi$ and $\alpha_1 = \alpha_2 = \alpha_3 = \alpha_4 = \alpha = 0$); a single fill-wall interface cohesion is considered ($c_1 = c_2 = c_3 = c_4 = c = 1$ kPa). For this illustrative example, the opening size is $B = 5$ m and $L = 10$ m. The fill internal friction angle, ϕ , is 35° , while the fill-wall friction angles are $\delta_1 = 10^\circ$, $\delta_2 = 20^\circ$, $\delta_3 = 30^\circ$, and $\delta_4 = 35^\circ$. The arching effect can be clearly observed for each case. All the graphs in Fig. 2 show that the stress magnitude in the fill is reduced, compared to overburden stresses, when depth increases. It can also be seen that the internal shear

stresses τ_B and τ_L are not nil (Fig. 2c), as would be the case for a single side wall friction angle δ . It can equally be seen that the vertical (Fig. 2a) and horizontal (Fig. 2b) stresses would be overestimated (for $\delta_1 = \delta_2 = \delta_3 = \delta_4 = 10^\circ$; upper limit) or underestimated (for $\delta_1 = \delta_2 = \delta_3 = \delta_4 = 35^\circ$; lower limit) if a single value of the fill-wall friction angle had been used.

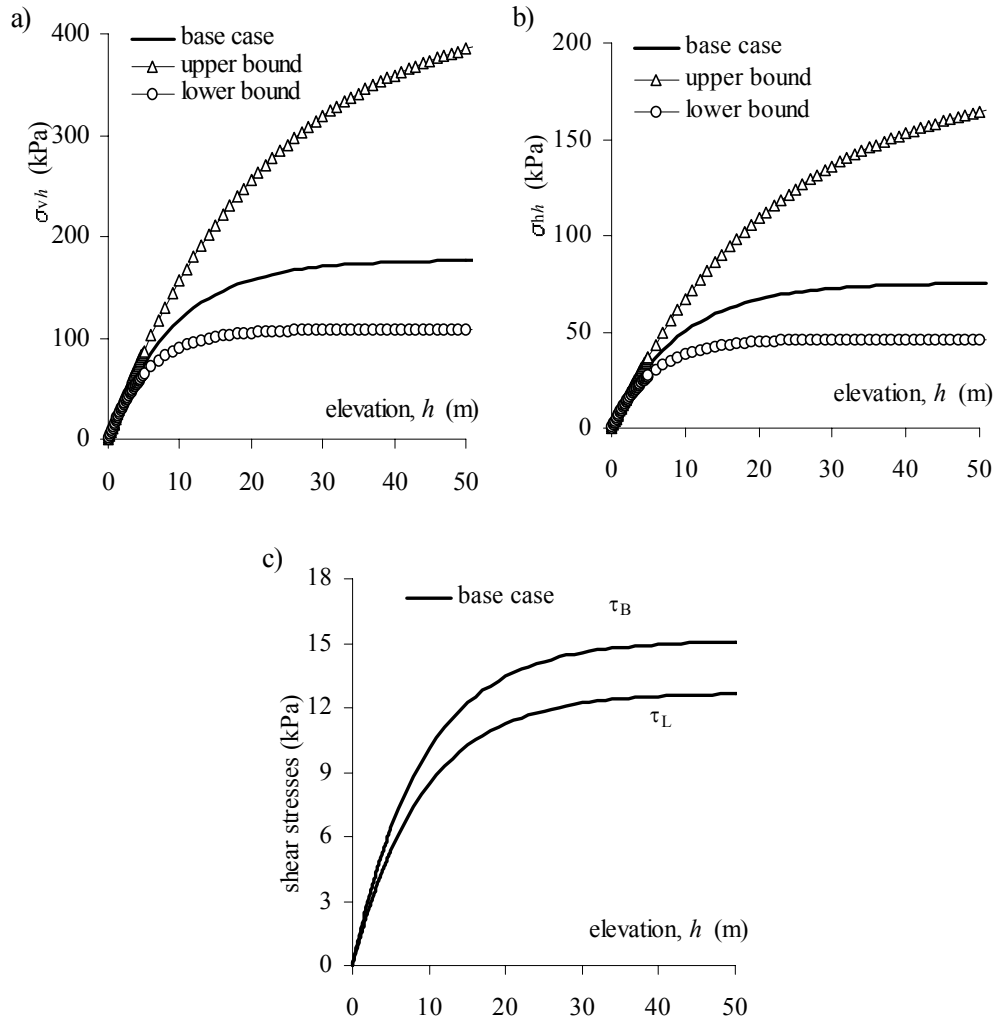


Fig. 2. Calculated values of vertical (a), horizontal (b), and shear (c) stresses versus elevation h ; $B = 5$ m, $L = 10$ m, $c_1 = c_2 = c_3 = c_4 = c = 1$ kPa, $\phi = 35^\circ$, $\gamma = 0.02$ MN/m³; the fill is at rest ($K_1 = K_2 = K_3 = K_4 = K = 1 - \sin\phi$ and $\alpha_1 = \alpha_2 = \alpha_3 = \alpha_4 = \alpha = 0$); three cases are concerned: a base case ($\delta_1 = 10^\circ$, $\delta_2 = 20^\circ$, $\delta_3 = 30^\circ$, $\delta_4 = 35^\circ$), the upper bound limit ($\delta_1 = \delta_2 = \delta_3 = \delta_4 = 10^\circ$) and the lower bound limit ($\delta_1 = \delta_2 = \delta_3 = \delta_4 = 35^\circ$).

Stress distributions are shown for the case where the reaction coefficient K_i is defined from the active (Fig. 3) and passive (Fig. 4) state. Under an active state, the vertical load at depth is larger than for the “at rest case” (compare Figs. 2 and 3). For the passive case (Fig. 4), the vertical (Fig. 4a), horizontal (Fig. 4b) and shear (Fig. 4c) stresses rapidly increase at small depth and become constant for a deeper opening. These stresses are much smaller than for the active and at rest cases, indicating a more developed arching effect in the backfilled opening.

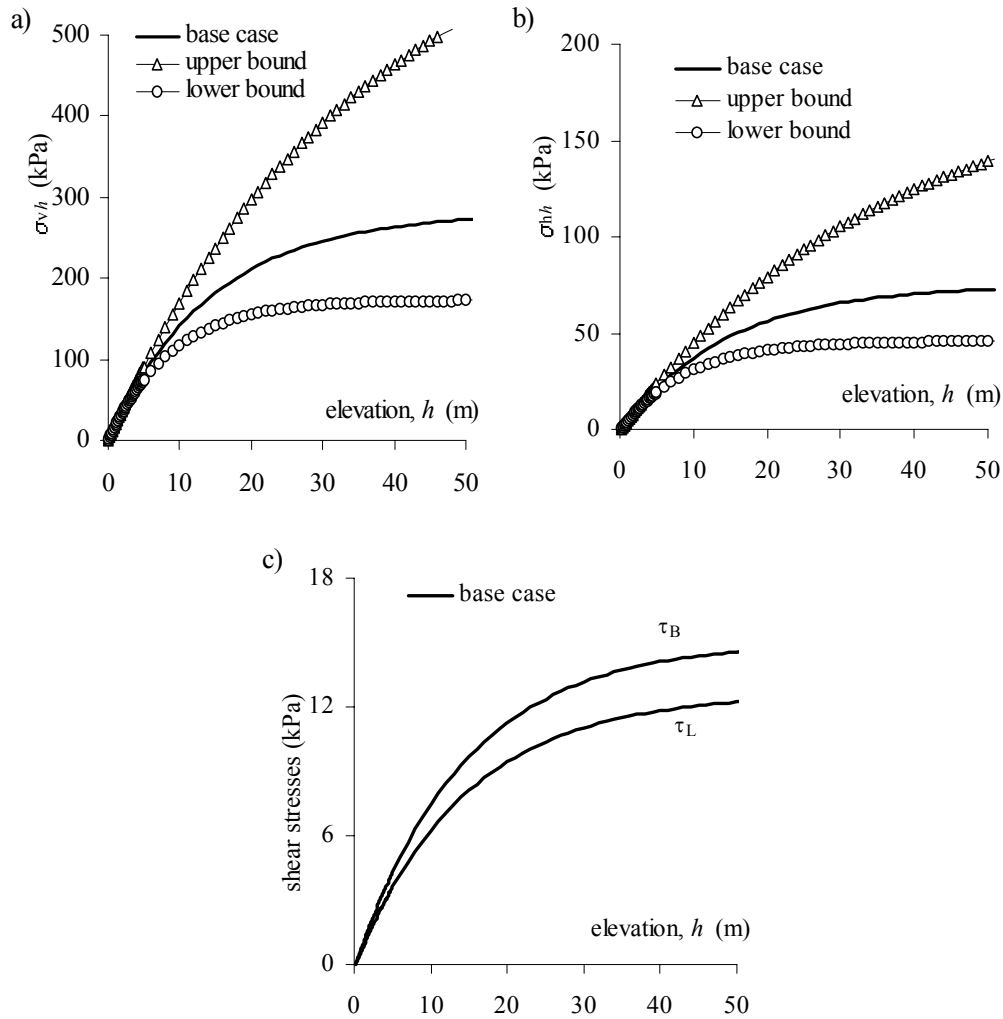


Fig. 3. Calculated values of vertical (a), horizontal (b), and shear (c) stresses versus elevation h ; $B = 5$ m, $L = 10$ m, $c_1 = c_2 = c_3 = c_4 = c = 1$ kPa, $\phi = 35^\circ$, $\gamma = 0.02$ MN/m³; the fill is in active state ($K_1 = K_2 = K_3 = K_4 = K$, $\alpha_1 = \alpha_2 = \alpha_3 = \alpha_4 = \alpha$; see Table 1); base case ($\delta_1 = 10^\circ$, $\delta_2 = 20^\circ$, $\delta_3 = 30^\circ$, $\delta_4 = 35^\circ$), upper bound limit ($\delta_1 = \delta_2 = \delta_3 = \delta_4 = 10^\circ$) and lower bound limit ($\delta_1 = \delta_2 = \delta_3 = \delta_4 = 35^\circ$).

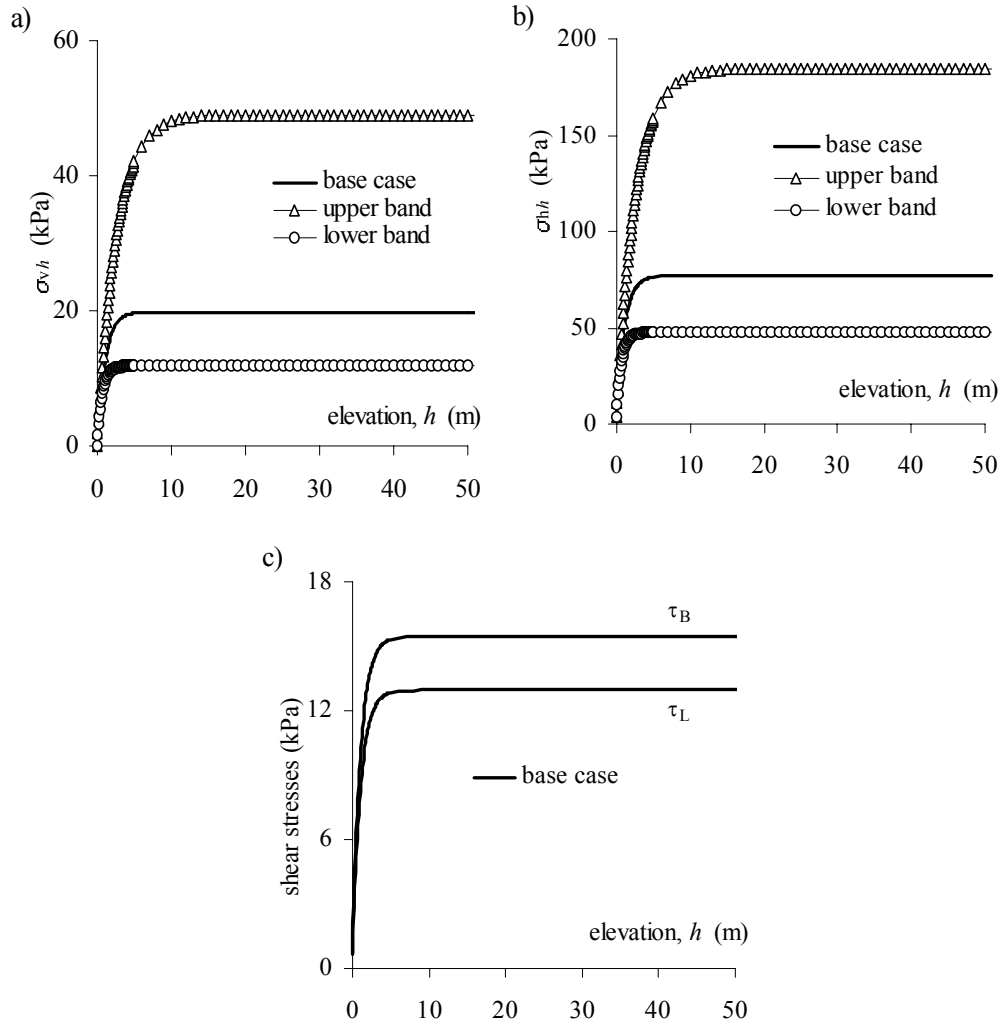


Fig. 4. Calculated values of vertical (a), horizontal (b), and shear (c) stresses versus elevation h ; $B = 5$ m, $L = 10$ m, $c_1 = c_2 = c_3 = c_4 = c = 1$ kPa, $\phi = 35^\circ$, $\gamma = 0.02$ MN/m³; the fill is in passive state ($K_1 = K_2 = K_3 = K_4 = K$, $\alpha_1 = \alpha_2 = \alpha_3 = \alpha_4 = \alpha$; see Table 1); base case ($\delta_1 = 10^\circ$, $\delta_2 = 20^\circ$, $\delta_3 = 30^\circ$, $\delta_4 = 35^\circ$), the upper bound limit ($\delta_1 = \delta_2 = \delta_3 = \delta_4 = 10^\circ$) and the lower bound limit ($\delta_1 = \delta_2 = \delta_3 = \delta_4 = 35^\circ$).

The influence of cohesion on the vertical (Fig. 5a), horizontal (Fig. 5b) and shear (Figs. 5c and 5d) stresses is shown in Fig. 5 for the case where the fill is at rest state ($K_1 = K_2 = K_3 = K_4 = K = 1 - \sin\phi$ and $\alpha_1 = \alpha_2 = \alpha_3 = \alpha_4 = \alpha = 0$). One can see that increasing the internal cohesion of fill decreases the stress magnitude; this is in accordance with field observations (e.g., Grice 1989).

Figure 6 illustrates the influence of the third dimension (the ratio of opening length to width $L:B = 5:3$) on the vertical stress σ_{vh} (Fig. 6a) and horizontal stress σ_{hh} (Fig. 6b). The stresses calculated with the three dimensional

solution (eq. [29]) are compared to those obtained with the two dimensional solution (eq. [30]). It shows that both the vertical and horizontal stress magnitudes are significantly overestimated by the two dimensional solution, and the overestimation increases with depth. Figure 7 shows that this overestimation becomes smaller when the opening is longer (at high $L:B$ ratio). The difference between the stress value provided by the two solutions depends on material properties (c , ϕ) and dimension of the openings (B , L , h) (see Discussion below).

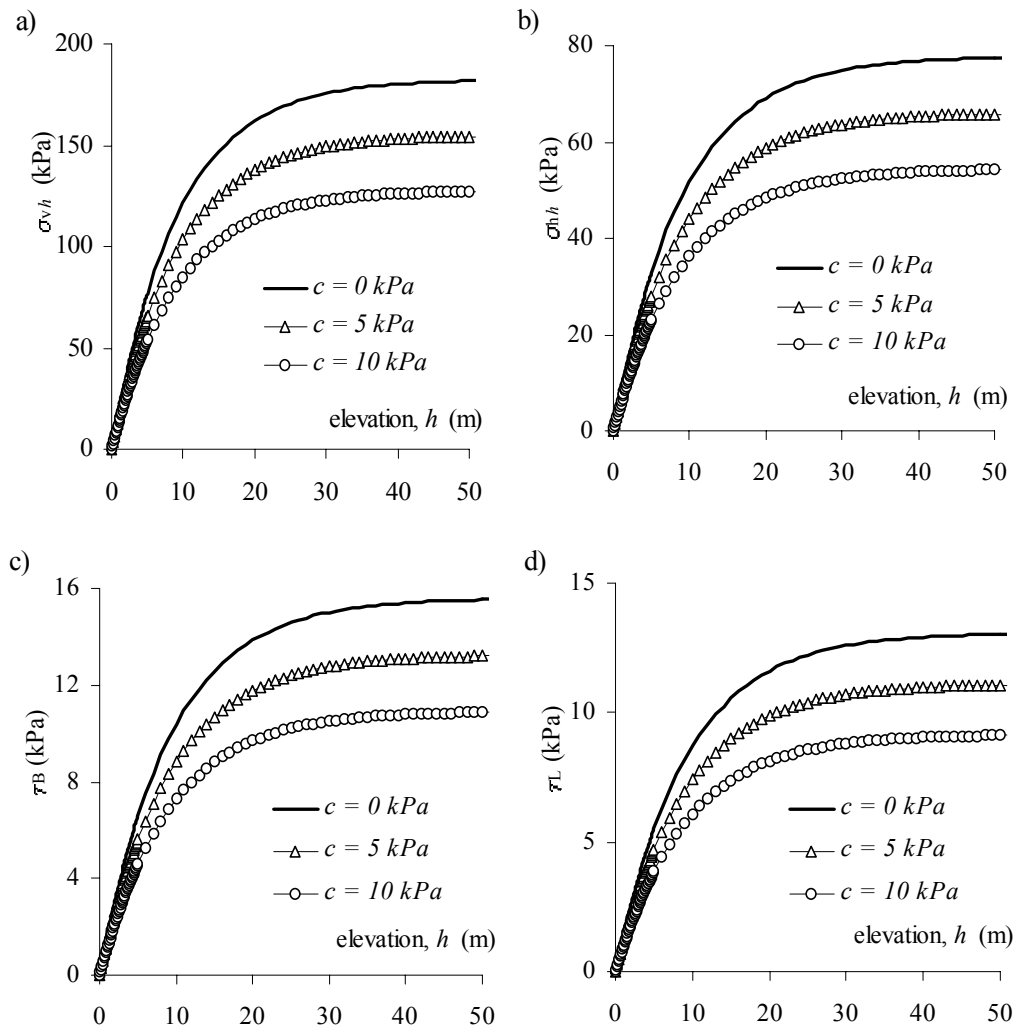


Fig. 5. Calculated values of vertical (a), horizontal (b), transverse (c), and longitudinal shear (d) stresses versus elevation h ; $B = 5$ m, $L = 10$ m, $\phi = 35^\circ$, $\gamma = 0.02$ MN/m³, $\delta_1 = 10^\circ$, $\delta_2 = 20^\circ$, $\delta_3 = 30^\circ$, and $\delta_4 = 35^\circ$; the fill is in at rest state (see Table 1).

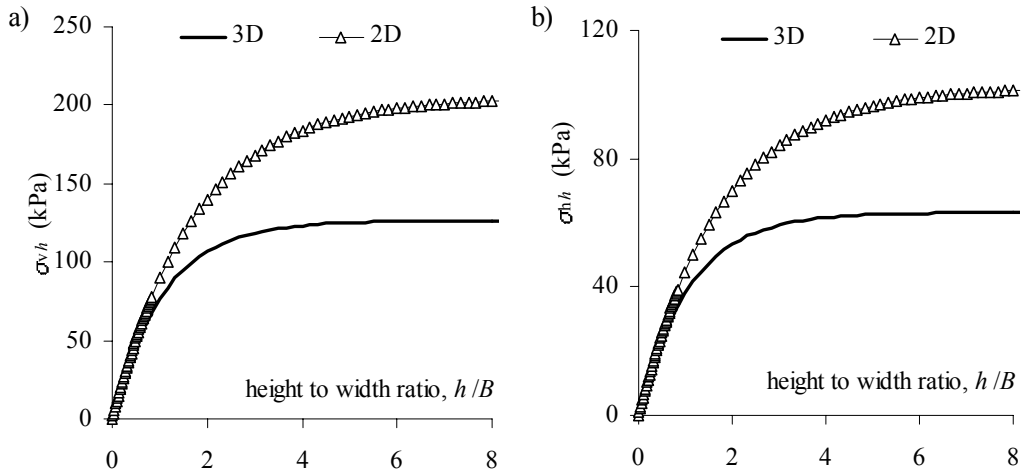


Fig. 6. Calculated values of vertical (a), horizontal (b) stresses versus the ratio h/B obtained using 2D (eq. [30]) and 3D (eq. [29]) solutions with the fill in at rest state (see Table 1); $B = 6$ m, $L = 10$ m, $c = 0.001$ MPa, $\delta = \phi = 30^\circ$, $K = 1 - \sin\phi = 0.5$, $\gamma = 0.02$ MN/m³.

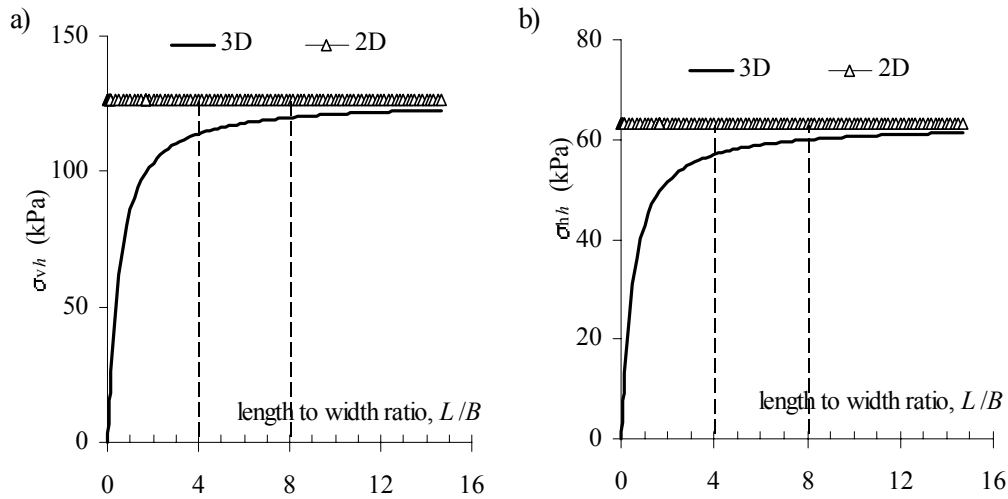


Fig. 7. Calculated values of vertical (a), horizontal (b) stresses versus length to width ratio L/B obtained using the 2D (eq. [30]) and 3D (eq. [29]) solutions with the fill in at rest state (see Table 1); $B = 6$ m, $h = 10$ m, $c = 0.001$ MPa, $\delta = \phi = 30^\circ$, $\gamma = 0.02$ MN/m³.

3. COMPARISON WITH NUMERICAL MODELING RESULTS

Numerical modeling results obtained by Li et al. (2003) with FLAC-2D (Itasca 2002) and a few new cases have been used for comparison purposes, to help assess the proposed analytical solutions. The geometry of the 2D opening, as well as the natural field stress state, and the rock mass and fill properties are shown in Fig. 8. The

rock mass is linearly elastic while the fill is modeled as a nonlinear elastoplastic Coulomb material. A one step mining and one step backfilling sequence is considered; hence, wall convergence occurs before the backfill is put in place.

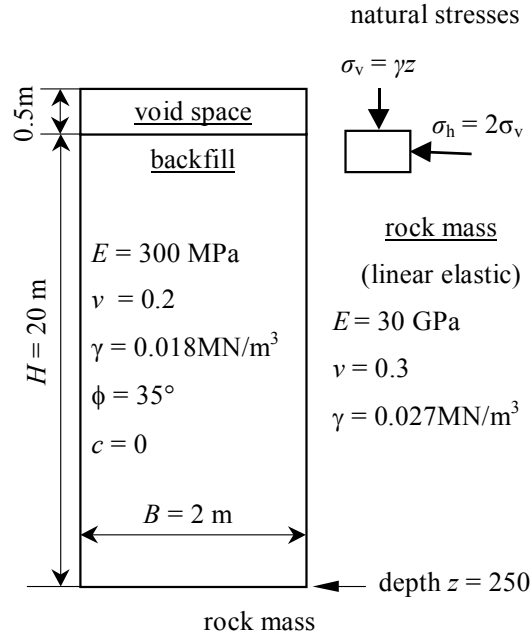


Fig. 8. Numerical model geometry of a narrow backfilled stope (not to scale) for FLAC-2D (Itasca 2002); the main properties for the rock mass and backfill are given using classical geomechanical notations.

For this 2D problem, the following equations are used to compare the analytical solution with some of the numerical modeling results:

$$[33] \quad \sigma_{vh} = \frac{\gamma B - \kappa_{13}}{\lambda_{13}} \left\{ 1 - \exp(-h\lambda_{13}B^{-1}) \right\}$$

with

$$[34] \quad \begin{aligned} \lambda_{13} &= K_1 (\tan\delta_1 + \tan\delta_3) \\ \kappa_{13} &= c_1 + c_3 + 2c(\tan\delta_1 + \tan\delta_3)\tan\alpha_1 \end{aligned}$$

Two cases are selected to illustrate the results for two sets of material parameters:

- 1) Granular fill: $c_1 = c_3 = c = 0$ kPa, $\delta_1 = \delta_3 = \phi = 35^\circ$. The results obtained from eqs. [19] and [33] and from the numerical model are shown in Fig. 9. With the analytical solution, the stresses are fairly similar when the

fill is considered at rest or in an active state (the passive state does not apply here). Arching effects are clearly visible, reducing the vertical stress gradient as depth is increased. In all simulations, the vertical stress is close to the vertical overburden stress (γh) at low depth, but it progressively deviates from this tendency to reach a plateau when h/B is high enough.

- 2) Granular fill, with different wall friction properties: $c_1 = c_3 = c = 0$ kPa, $\delta_1 = 25^\circ$, $\delta_3 = \phi = 35^\circ$. In this case, shear stress appears in the horizontal planes. As seen in Fig. 10, the proposed equations (with $K = K_0$ and K_a) appear suitable for this case (see Figs. 10a, b, c), accounting for the internal shear stress in the fill. Although the numerical and analytical results shown in Fig. 10 (and others; not presented here) are not identical, they show the same tendencies with about the same stress magnitudes. Considering the basic assumptions and simplifications made with the numerical modeling (e.g., Aubertin et al. 2003; Li et al. 2003), the correspondence between the two sets of results is deemed satisfactory for this preliminary assessment.

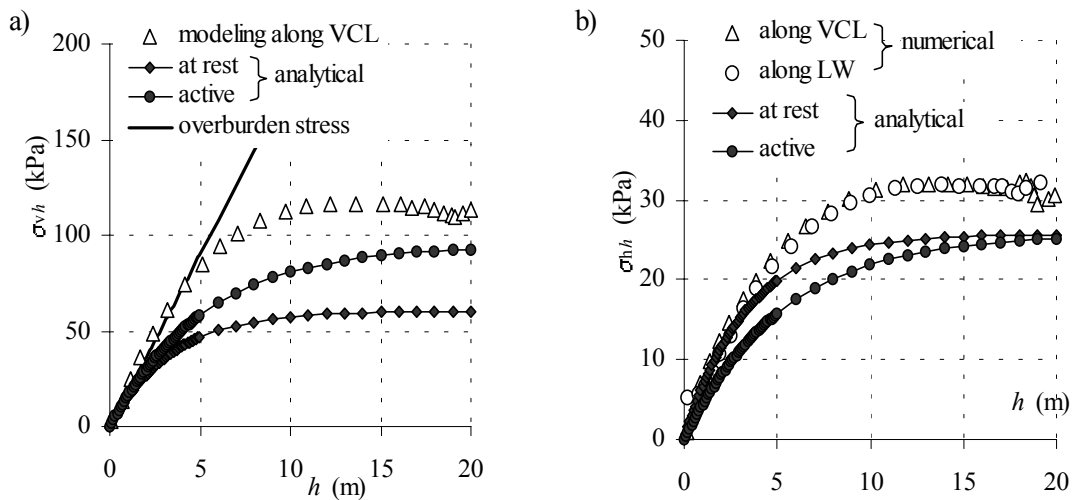


Fig. 9. Comparison of vertical (a), and horizontal (b) stresses along the vertical central line (VCL) and left wall (LW) obtained from the numerical modeling and the analytical solutions, with $c_1 = c_3 = c = 0$ kPa, $\delta_1 = \delta_3 = \phi = 35^\circ$.

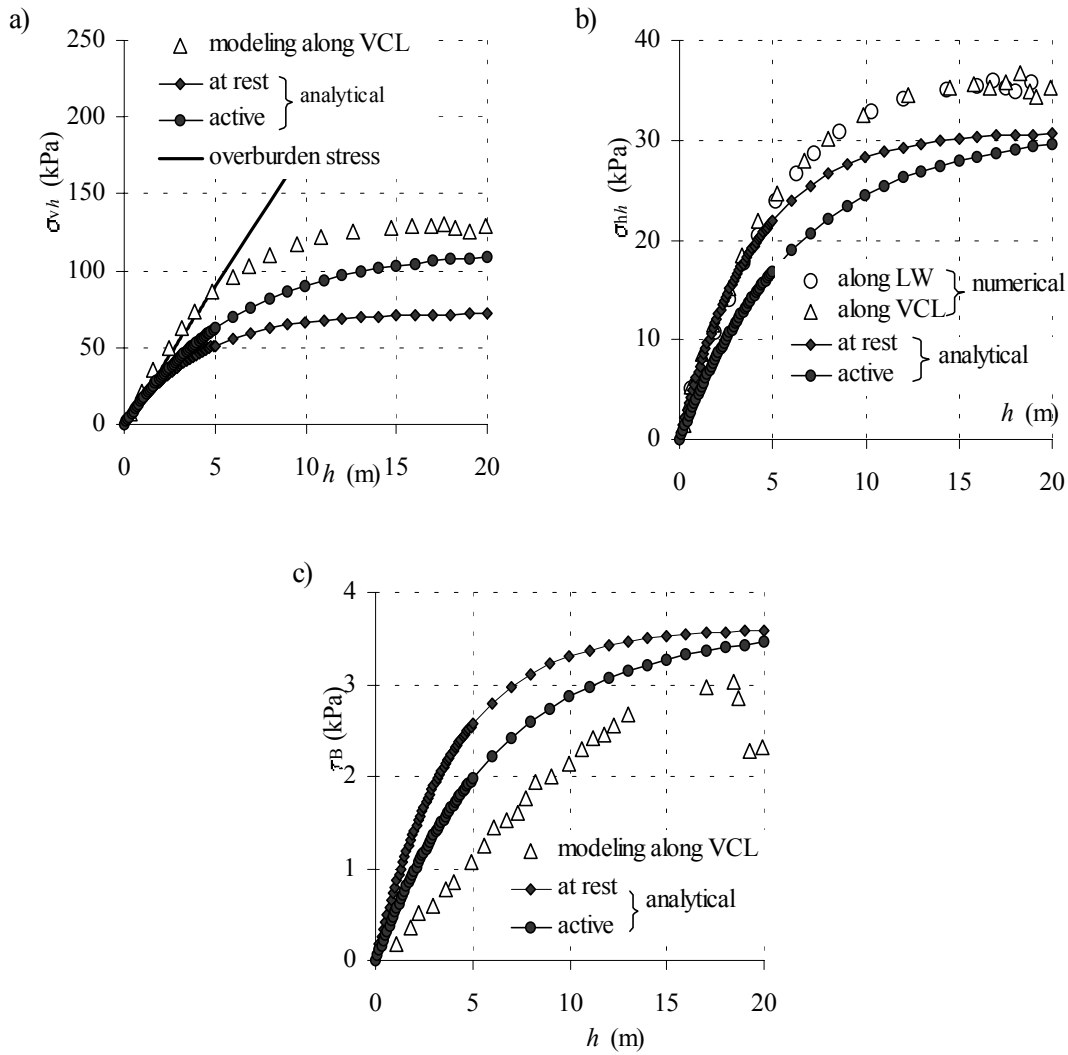


Fig. 10. Comparison between the numerical model and the analytical solutions for vertical (a), horizontal (b) and shear (c) stresses versus the opening height, with $c_1 = c_3 = c = 0$ kPa, $\delta_1 = 25^\circ$, $\delta_3 = \phi = 35^\circ$.

4. APPLICATION TO LABORATORY DATA

Centrifuge test results were reported by Take and Valsangkar (2001). In these experiments, earth pressure cells were mounted inside a backfilled box with aluminum walls. To investigate the effect of boundaries with dissimilar frictional characteristics, one of the aluminum surfaces was covered with a sheet of 120A-grit sandpaper (Take 1998). The backfill used in these tests was a poorly graded sand with little or no fines. The maximum and minimum dry densities were 1.62 and 1.34 g/cm³, respectively. Angles of internal friction (ϕ) and interface friction (δ) angles are given in Table 2. The centrifuge experiments were performed at an acceleration

of $35.7g$ (g is the gravity acceleration) to simulate a 5 m high retaining wall prototype. With this acceleration, the equivalent unit weight of the dense backfill (having a 79% relative density) is 0.554 MN/m^3 , while that of the loose backfill (34% relative density) becomes 0.508 MN/m^3 . Table 3 gives the conditions and parameters for the different cases.

Table 2. Internal (ϕ) and interface (δ) friction angles for the backfill (after Take and Valsangkar 2001).

	Loose backfill (34% relative density, density 1.42 g/cm^3)	Dense backfill (79% relative density, density 1.55 g/cm^3)
ϕ backfill	30°	36°
δ backfill and aluminium	23°	25°
δ backfill and sandpaper	32°	36°

Table 3. Parameters used in the calculation results presented in Figs. 11 – 13, base on data taken from Take and Valsangkar (2001).

Figure	Backfill	Geometry $B \text{ (cm)} \times L \text{ (cm)}$	Fill parameters			Wall-fill friction angle [‡] ($^\circ$)			
			c	γ^\dagger	$\phi \text{ (}^\circ\text{)}$	δ_1	δ_2	δ_3	δ_4
11a	dense	18.4×25.4	0	0.554	36	25	25	25	25
11b	dense	7.5×25.4	0	0.554	36	25	25	25	25
11c	dense	3.8×25.4	0	0.554	36	25	25	25	25
11d	dense	1.5×25.4	0	0.554	36	25	25	25	25
12a	dense	18.4×25.4	0	0.554	36	25	36	25	25
12b	dense	7.5×25.4	0	0.554	36	25	36	25	25
12c	dense	3.8×25.4	0	0.554	36	25	36	25	25
12d	dense	1.5×25.4	0	0.554	36	25	36	25	25
13a	loose	3.8×25.4	0	0.508	30	23	32^\ddagger	23	23
13b	loose	1.5×25.4	0	0.508	30	23	32^\ddagger	23	23

[†] Values obtained by multiplying the backfill density by the centrifuge acceleration (in MN/m^3);

[‡] The backfill friction angle, ϕ , is used when the wall-fill friction angle δ is higher than ϕ .

A first series of tests was conducted on dense backfill. The walls were not covered, so $\phi = 36^\circ$, $\delta_1 = \delta_2 = \delta_4 = \delta_3 = 25^\circ$. Figure 11 shows the comparison between the experimental results and the proposed analytical solution (eqs. [19] and [29]). At rest (K_0) and active (K_a) states are considered here ($K_1 = K_2 = K_3 = K_4 = K$ and $\alpha_1 = \alpha_2 = \alpha_3 = \alpha_4 = \alpha$; see Table 1 for values of K and α). The horizontal stress based on the overburden calculation is also plotted for the four geometries considered ($L = 25.4$ cm and $B = 1.5, 3.8, 7.5$ and 18.4 cm; see Table 3). The proposed analytical solution describes the experimental results quite well, and confirms the existence of stress transfer to the abutment (due to the arching effect).

Another series of tests was performed by Take and Valsangkar (2001) with this same dense backfill, with wall 2 covered with sandpaper to simulate a rough surface. In this case, $\phi = 36^\circ$, $\delta_1 = \delta_3 = \delta_4 = 25^\circ$, $\delta_2 = 36^\circ$. There were no solutions available to analyze this type of test which includes two different fill-wall friction angles. Take and Valsangkar (2001) used two dimensional calculations with upper and lower parameter bounds to compare to their experimental results. Here, the proposed general analytical solution (eqs. [18] and [19]) is used to evaluate this situation in more detail. Figure 12 shows a comparison between the experimental results and the proposed solution for at rest and active states ($K_1 = K_2 = K_3 = K_4 = K$ and $\alpha_1 = \alpha_2 = \alpha_3 = \alpha_4 = \alpha$; see Table 1 for values of K and α). Again, the newly developed equations describe the experimental results well (with the parameters given in Table 3).

Take and Valsangkar (2001) have also conducted a series of tests with loose backfill (34% relative density). The model rock face (wall 2) was again covered with sandpaper to simulate a rough surface. The friction angles are $\phi = 30^\circ$, $\delta_1 = \delta_3 = \delta_4 = 23^\circ$, $\delta_2 = 32^\circ$. As indicated previously, when the fill-wall friction angle is larger than the fill material friction angle ϕ , the latter is used for the interface, so $\delta_2 = \phi = 30^\circ$ is adopted here (see Table 3). Again, the proposed general solution (eqs. [18] and [19]) with an active or an at rest state ($K_1 = K_2 = K_3 = K_4 = K$ and $\alpha_1 = \alpha_2 = \alpha_3 = \alpha_4 = \alpha$; see Table 1 for values of K and α) gives a fairly good prediction of the experimental results (Fig. 13).

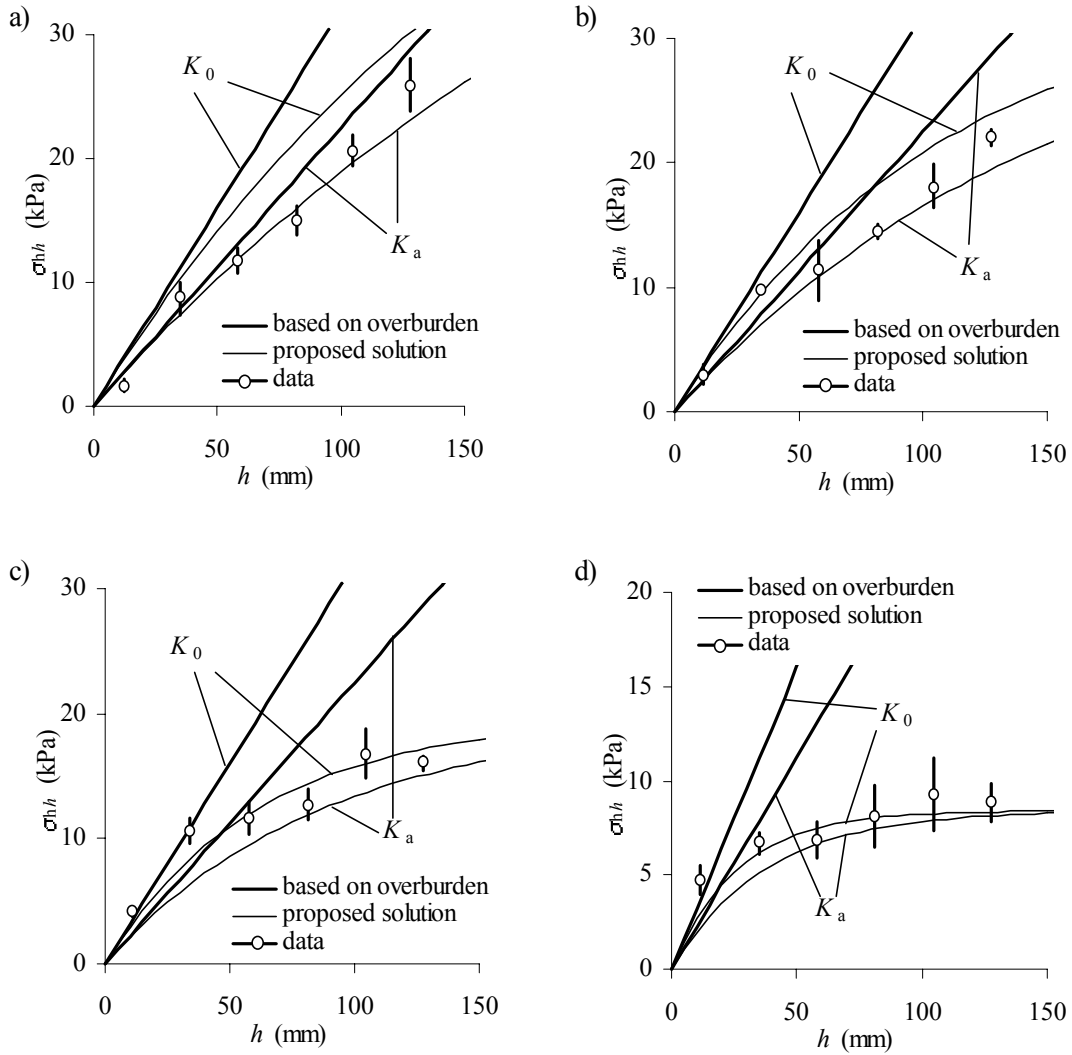


Fig. 11. Comparison between the proposed solution (eqs. [19] and [29]) and experimental results obtained on 3D physical model backfilled with dense sand (data taken from Take and Valsangkar 2001; see text for details).

5. EXTENSION TO CYLINDRICAL BINS

When the walls of the opening are made of one type of material, the proposed solution (eq. [18] or [29]) can be (in principal) extended to other cross section shapes, using the following equations:

$$[35] \quad 2(L + B) = P$$

$$[36] \quad L \cdot B = A$$

where A is the cross sectional area and P is its perimeter. Introducing eqs. [35] and [36] into eq. [29], one obtains:

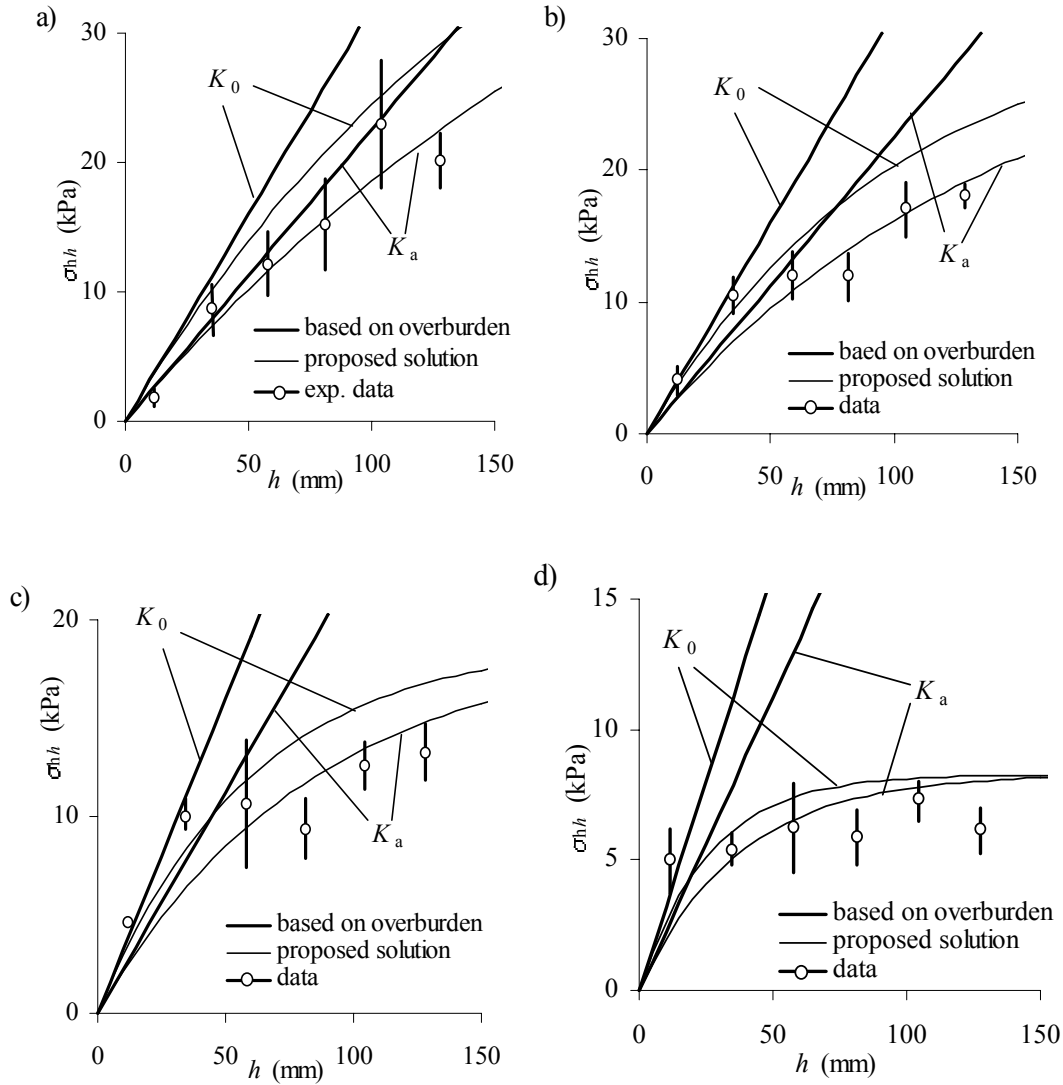


Fig. 12. Comparison between the proposed general solution (eq. [18] and [19]) and the experimental results obtained on a 3D physical model backfilled with dense sand (data taken from Take and Valsangkar 2001; see text for details).

$$[37] \quad \sigma_{vh} = \frac{\gamma A / P - c(1 + 2 \tan \alpha \tan \delta)}{K \tan \delta} \left\{ 1 - \exp(-KhPA^{-1} \tan \delta) \right\}$$

This equation reduces to Janssen's formula for $c = 0$ (Cowin 1977). If the cross section is circular with a diameter D , eq. [37] becomes:

$$[38] \quad \sigma_{vh} = \frac{\gamma D / 4 - c(1 + 2 \tan \alpha \tan \delta)}{K \tan \delta} \left\{ 1 - \exp(-4KhD^{-1} \tan \delta) \right\}$$

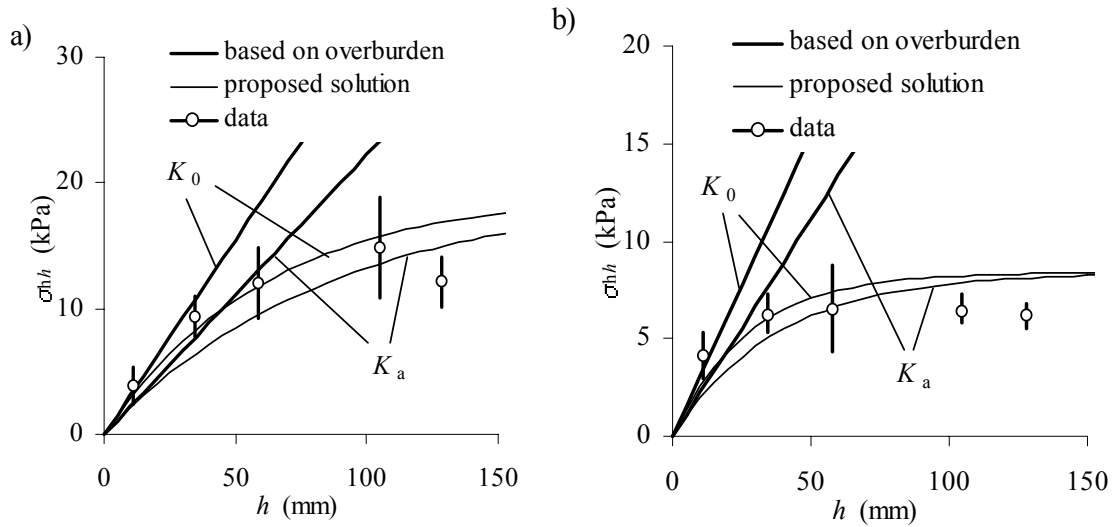


Fig. 13. Comparison between the proposed solution (eqs. [18] and [19]) and experimental results obtained on a 3D physical model backfilled with loose sand (data taken from Take and Valsangkar 2001; see text for details).

Figs. 14 to 16 show a comparison between experimental results obtained in silos and the proposed analytical solution (eq. [38]) with $K = K_0$ (at rest state) and K_a (active state). Material properties and parameters used here are taken from Blight (1986a, b) and are given in Table 4. One can see that the proposed solution reproduces the experimental results well.

Table 4. Parameters used in the calculation results presented in Figs. 14 – 16, base on data taken from Blight (1986a, b).

Figure	Backfill	Wall	D (m)	c	γ (kN/m ³)	ϕ (°)	δ (°)	Reference
14	coal	concrete	20	0	8.1	40	36	Blight 1986a
15	wheat and barley	concrete	7	0	7.8	24	24	Hartlen et al. 1984
16	fine powder	-----	15	0	11.5	38	36	Blight 1986b

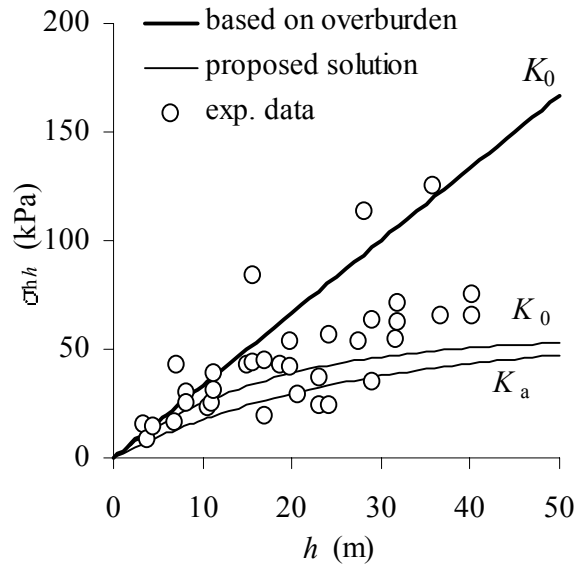


Fig. 14. Comparison between the proposed solution (eq. [38]) and the experimental measurements made in coal load-out silo; $D = 20$ m (data taken from Fig. 6 in Blight 1986a).

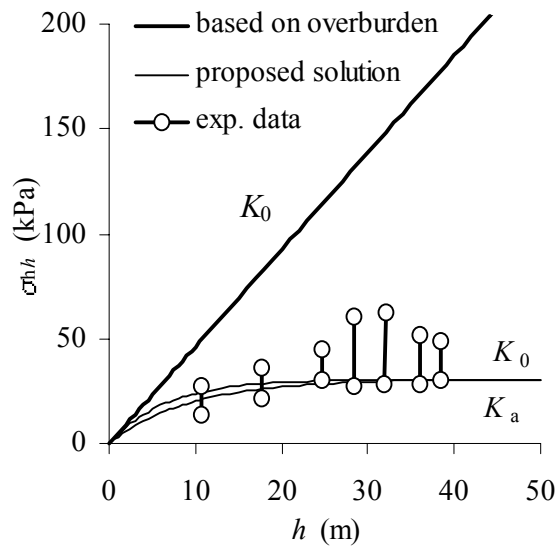


Fig. 15. Comparison between the proposed solution (eq. [38]) and the experimental measurements made in a grain silo; $D = 7$ m (data taken from Fig. 9 in Blight 1986a).

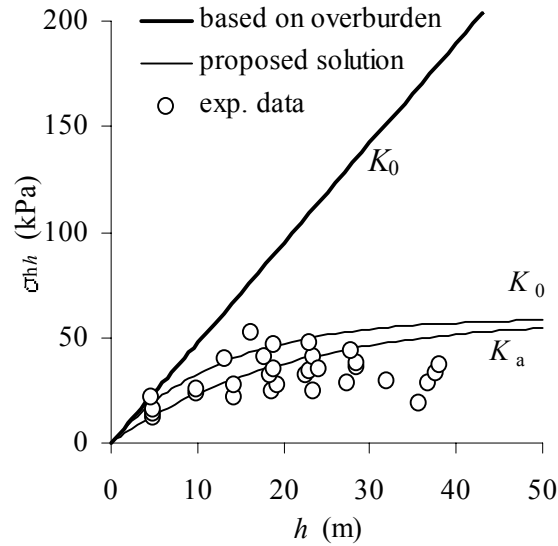


Fig. 16. Comparison between the proposed solution (eq. [38]) and the experimental measurements made in a fine powder silo; $D = 15$ m (data taken from Fig. 5 in Blight 1986b).

6. DISCUSSION

A general 3D analytical solution (eqs. [18], [19] and [23]) has been developed based on the arching theory, using the Marston solution as a starting point. The proposed solution has been shown in the previous sections to provide representative estimates for the earth pressures in backfilled openings with four walls having different interface properties. However, the potential user should keep in mind that this analytical solution is based on some simplifying assumptions. Some key aspects are recalled below.

The analytical solutions presented above (eqs. [18], [19] and [23]) are based on the approach proposed by Marston (1930) and co-workers, which has been extended here for generalized 3D conditions. The approach divides the narrow, vertical backfilled opening into thin horizontal layer elements on which acts a uniform state of stress. The contact stress between the fill and walls is expressed as a function of the coefficient of lateral earth pressure K_{ci} ($i = 1$ to 4). When the wall does not move, an 'at rest' condition can be adopted to define K_{ci} ($= K_0$, see eq. [6]). However, for cases where an outward displacement is expected to occur at the interface, the value of K_{ci} has become a topic of investigation and discussion for many arching problems (e.g., Krynine 1945; Handy 1985, 2004; Blight 1986a; Frydman and Keissar 1987; Harrop-Williams 1989; Iglesia et al. 1999).

In many practical applications of arching equations ensuing from Janssen's (1895) basic theory, problems with outward movement of the walls have been linked to active earth pressure conditions, so the Rankine active earth pressure coefficient is often used (i.e. $K_{ci} = K_a$). The use of K_a is, however, known to be strictly (theoretically) incorrect as the Rankine active coefficient defines the ratio of the principal stresses σ_3/σ_1 (where σ_3 and σ_1 are the minor and major principal stress, respectively). For an opening backfilled with a soft, yielding material, shearing along the interface induces a rotation of the stresses. Thus, the horizontal and vertical stresses acting on the wall are not the principal stresses if a shear stress is induced (as is expected to occur with frictional materials).

Both analytical solutions and numerical modeling results show that there is indeed a rotation of the principal stresses, and that the stresses are not distributed uniformly in the horizontal layer element (e.g., Handy 1985; Li et al. 2003).

Data presented by Frydman and Keissar (1987) show that the value of the $\sigma_h/(\gamma h)$ ratio (horizontal stress over vertical overburden pressure) is typically close to K_0 near the surface of the fill, and progressively decreases with depth to values below K_a (down to about 1/3 to 1/2 K_a). This would tend to indicate that adopting $K_{ci} = K_a$ would overestimate σ_h . However, with the approach proposed here, K_{ci} has been defined by the ratio of the horizontal (σ_{hh}) to vertical (σ_{vh}) stress at a given position h . In this definition of K_{ci} , the value of σ_{vh} is obtained from the arching equation, so it can be much smaller than the overburden weight of the fill column. Comparisons made with both numerical and experimental results tend to indicate that the calculated value of σ_{hh} is generally close to the expected value. Hence, the simplifying assumptions adopted to develop the analytical solutions and to define K_{ci} are seen to provide realistic estimates of the earth pressure on the boundaries.

Considering the other uncertainties encountered in such types of geotechnical applications (including opening geometry and material properties), the proposed solution is hence considered an acceptable compromise with more rigorous definitions of earth pressure (when K_0 or K_a are used for K_{ci}).

A similar argument could be made for conditions where there is an inward displacement of the walls. This could be the case, for example, with cut and fill stopes excavated and backfilled progressively. In such

situations, depending on the amount of wall convergence and backfill compression, the confined fill can even be submitted to a horizontal pressure that exceeds the value obtained from a Rankine passive coefficient K_p (e.g. Aubertin et al. 2003). This aspect, however, requires more work before it can be assessed more completely, as wall sizes, interface properties, and filling sequence are known to have a large influence on such passive earth pressure (e.g., Bransby and Smith 1975; Li et al. 2003).

Another aspect that will require more work is the influence of pore pressure under saturated and unsaturated conditions, and backfill material response in confined openings.

Finally, even if the solution proposed here was developed for vertical openings, it could also be applicable for sub-vertical openings when the stresses on each side have about the same magnitude (e.g., Knutsson 1981). A more complete extension to inclined openings is nevertheless needed for general applications and has been object of publications (e.g., James et al. 2004; Li et al. 2005).

7. CONCLUSION

The stress components in backfilled openings are affected not only by the weight of the fill, but also by interaction between the fill and the opening walls. Some of the stress in the backfill is thus transferred to the adjacent walls through shearing forces between the fill and walls. This leads to a decrease of stress in the fill compared to the overburden stress. This phenomenon is known as the arching effect.

Based on the arching theory, a three-dimensional analytical solution was developed using the Marston method as a starting point to evaluate the earth pressures in narrow, vertical backfilled openings. Both the 3D opening geometry and the fill-wall interface properties were taken into account. It has been shown that pressure estimations which ignore different shear properties along the four walls of the opening may generate some significant errors. The proposed solution can, however, provide representative estimates for the earth pressures in backfilled openings with four walls having different interface properties. It has also been shown that the opening length has a significant influence on the earth pressure in the backfill. The length to width ratio at which the 2D solution becomes significantly different from the 3D solution is a function of opening size and material property. The proposed solution was further extended to other cross sectional openings, including cylindrical

bins. The versatility and descriptive capability of the proposed solution were demonstrated by comparison with a numerical model and with experimental results taken from the literature. The proposed analytical solution can thus be used, at a preliminary phase, to estimate the earth pressure in narrow, vertical backfilled openings, including mining stopes, trenches, bins or silos.

ACKNOWLEDGEMENT

The authors acknowledge the financial support from the Institut de Recherche Robert-Sauvé en Santé et en Sécurité du Travail du Québec (IRSST) and from the participants of the Industrial NSERC Polytechnique-UQAT Chair (<http://www.polymtl.ca/enviro-geremi/>). The authors thank John Molson and Michael James for their review of this manuscript.

REFERENCES

- Atkinson, J.H., Cairncross, A.M., James, R.G. 1974. Model tests on shallow tunnels in sand and clay. *Tunnels and Tunnelling*, **6**(4): 28-32.
- Aubertin, M. 1999. Application de la mécanique des sols pour l'analyse du comportement des remblais miniers souterrains. Short Course (unpublished lecture notes), 14^e Colloque en Contrôle de Terrain, Val-d'Or, 23-24 mars 1999. Association Minière du Québec.
- Aubertin, M., Bussière, B., Bernier, L. 2002. Environnement et gestion des rejets miniers. Manual on CD-ROM, Presses Internationales Polytechniques.
- Aubertin, M., Li, L., Simon, R. 2000. A multiaxial stress criterion for short term and long term strength of isotropic rock media. *International Journal of Rock Mechanics and Mining Sciences*, **37**: 1169-1193.
- Aubertin, M., Li, L., Arnoldi, S., Belem, T., Bussière, B., Benzaazoua, M., Simon, R. 2003. Interaction between backfill and rock mass in narrow stopes. *In* P.J. Culligan, H.H. Einstein, A.J. Whittle (eds), *Soil and Rock America 2003*, vol. 1, pp. 1157-1164. Essen: Verlag Glückauf Essen (VGE).
- Belem, T., Harvey, A., Simon, R., Aubertin, M. 2004. Measurement and prediction of internal stresses in an underground opening due to backfilling with cemented paste. Fifth International Symposium on Ground Support in Mining and Underground Construction: Ground Support 2004, 28-30 September 2004, Perth, Western Australia.

- Blight, G.E. 1986a. Pressure exerted by materials stored in silos: part I, coarse materials. *Géotechnique*, **36**(1): 33-46.
- Blight, G.E. 1986b. Pressure exerted by materials stored in silos: part II, fine powders. *Géotechnique*, **36**(1): 47-56.
- Bowles, J.E. 1988. *Foundation Analysis and Design*. McGraw-Hill.
- Bransby, P. L., Smith, A.A. 1975. Side friction in model retaining-wall experiments. *Journal of Geotechnical Engineering Division*, **101**(GT7): 615-632.
- Brechtel, C.E., Struble, G.R., Guenther, B. 1999. The evaluation of cemented rockfill spans at the Murray mine. *In* B. Amadei, Kranz, Scott, Smeallie (eds.), *Rock Mechanics for Industry*, vol. 1, pp. 481-487. Rotterdam: Balkema.
- Brummer, R.K., Gustas, R., Landriault, D.A., Steed, C.M. 1996. Mining under backfill - Field measurements and numerical modelling. *In* M. Aubertin, F. Hassani, H. Mitri (eds.), *Rock Mechanics: Tools and Techniques*, pp. 269-276. Rotterdam: A.A. Balkema.
- Chen, W.F., Liu, X.L. 1990. *Limit analysis in soil mechanics*. Amsterdam: Elsevier.
- Cowin, S.C. 1977. The theory of static loads in bins. *Journal of Applied Mechanics*, **44**: 409-412.
- Frydman, S.F., Keissar, I. 1987. Earth pressure on retaining walls near rock mass faces. *Journal of Geotechnical Engineering, ASCE*, **113**(6): 586-599.
- Grice, A.G. Fill research at Mount Isa Mines Limited. *In* F.P. Hassani, M.J. Scoble and T.R. Yu (eds.), *Innovations in Mining Backfill Technology; Proceedings of the 4th International Symposium on Mining with Backfill*, Montreal, 2-5 October 1989, pp.15-22. Rotterdam: A.A. Balkema, The Netherlands.
- Handy, R.L. 1985. The arch in soil arching. *Journal of Geotechnical Engineering, ASCE*, **111**(3): 302-318.
- Handy, R.L. 2004. Anatomy of an error. *Journal of Geotechnical and Geoenvironmental Engineering*, **130**(7): 768-771.
- Harrop-Williams, K. 1989. Arch in soil arching. *Journal of Geotechnical Engineering*, **115**(3): 415-419.
- Hartlen, J., Nielsen, J., Ljunggren, L. 1984. The wall pressure in large grain silos. Swedish Council for Building Research, Stockholm.
- Harvey, A. 2004. Étude comparative des contraintes triaxiales dans le remblai en pâte selon la portée des chantiers. M.Sc.A. thesis, École Polytechnique de Montréal.
- Hassani, F., Archibald, J.H. 1998. *Mine Backfill*. CIM, CD-ROM.
- Hassani, F., Fotoohi, K. 1997. Quantitative evaluation of pastefill performance to alleviate rock burst. Séminaire sur l'Emploi du Remblai en Pâte dans les Mines Souterraines, Bibliothèque Nationale du Québec, vol. 1, pp. 65-77.
- Hunt, R. E. 1986. *Geotechnical engineering analysis and evaluation*. McGraw-Hill, New York.

- Hustrulid, W., Qianyan, Y., Krauland, N. 1989. Modeling of cut-and-fill mining systems – Näsleden revisited. *In* F.P. Hassani, M.J. Scoble, T.R. Yu (eds), *Innovation in Mining Backfill Technology*, pp. 147-164. Rotterdam: Balkema.
- Iglesia, G.R., Einstein, H.H., Whitman, R.V. 1999. Determination of vertical loading on underground structures based on an arching evolution concept. *In* C. Fernandez, R.A. Bauer (eds.), *Geo-Engineering for Underground Facilities*, pp. 495-506. Geo-Institute of ASCE.
- Itasca, 2002. *FLAC - Fast Lagrangian Analysis of Continua, User's Guide*. Minneapolis, MN: Itasca Consulting Group, Inc.
- Jaeger, J.C., Cook, N.G.W. 1979. *Fundamentals of rock mechanics: Third edition*. Chapman and Hall, New York.
- Jaky, J. 1948. Pressure in silos. *Proceedings of the 2nd International Conference on Soil Mechanics and Foundation Engineering*, vol. 1, pp. 103-107. Rotterdam: Balkema.
- Janssen, H.A. 1895. Versuche über Getreidedruck in Silozellen. *Zeitschrift Verein Ingenieure*, **39**: 1045-1049.
- James, M., Li, L., Aubertin, M. 2004. Evaluation of the earth pressures in backfilled stopes using limit equilibrium analysis. 57th Canadian Geotechnical Conference and the 5th joint CGS-IAH Conference, Quebec city, October 24-27, 2004.
- Jung, S.J, Biswas, K 2002. Review of current high density paste fill and its technology. *Mineral Resources Engineering*, **11**(2): 165-182.
- Krynine, D.P. 1945. Discussion of “Stability and stiffness of cellular cofferdams” by Karl Terzaghi. *Transaction of ASCE*, **110**: 1175-1178.
- Knutsson, S. 1981. Stresses in the hydraulic backfill from analytical calculations and in-situ measurements. *In* O. Stephansson, M.J. Jones (eds), *Proceedings of the Conference on the Application of Rock Mechanics to Cut and Fill Mining*: 261-268. Institution of Mining and Metallurgy.
- Kump, D. 2001. Backfill - Whatever it takes. *Mining Engineering*, **53**(1): 50-52.
- Kutzner, C. 1997. *Earth and rockfill dams: Principles of design and construction*. Rotterdam: Balkema.
- Ladanyi, B., Hoyaux, B. 1969. A study of the trap-door problem in a granular mass. *Canadian Geotechnical Journal*, **6**(1): 1-14.
- Landriault, D.A., Brown, R.E., Counter, D.B. 2000. Paste backfill study for deep mining at Kidd Creek. *CIM Bulletin* , **93**(1036): 156-161.
- Li, L., Aubertin, M., Simon, R., Bussière, B., Belem, T. 2003. Modeling arching effects in narrow backfilled stopes with FLAC. *In* R. Brummer, P. Andrieux, C. Detournay, R. Hart (eds.), *FLAC and Numerical Modeling in Geomechanics – 2003*, pp. 211-219. Lisse: A.A Balkema.

- Li, L., Aubertin, M., Belem, T., Simon, R., James, M., Bussière, B. 2004. A 3D analytical solution for evaluating earth pressures in vertical backfilled stopes. 57th Canadian Geotechnical Conference and the 5th joint CGS-IAH Conference, Quebec city, October 24-27, 2004.
- Li, L., Aubertin, M., James, M. 2005. A semi-analytical method to evaluate earth pressures in backfilled vertical and inclined stopes. *International Journal for Numerical and Analytical Methods in Geomechanics* (submitted).
- Marston, A. 1930. The theory of external loads on closed conduits in the light of latest experiments. Bulletin No. 96, Iowa Engineering Experiment Station, Ames, Iowa.
- McCarthy, D.F. 1988. *Essentials of Soil Mechanics and Foundations: Basic Geotechnics*. Prentice Hall.
- Mitchell, R.J. 1983. *Earth structures engineering*. Boston: Allen & Unwin.
- Pariseau, W.G. 1981. Finite-element method applied to cut and fill mining. *In* O. Stephansson, M.J. Jones (eds.), *Application of Rock Mechanics to Cut and Fill Mining: Proceedings of the Conference on the Application of Rock Mechanics to Cut and Fill Mining*, June 1-3, 1980, Lulea, pp. 284-292. Institution of Mining and Metallurgy.
- Richards, J.C. 1966. *The Storage and Recovery of Particulate Solids*. Institution of Chemical Engineers, London.
- Richmond, O., Gardner, G.C. 1962. Limiting spans for arching of bulk materials in vertical channels. *Chemical Engineering Science*, vol. 17, pp. 1071-1078.
- Spangler, M.G. 1948. Underground conduits – An appraisal of modern research. *Transactions, American Society of Civil Engineers*, **113**: 316-374.
- Spangler, M.G., Handy, R.L. 1984. *Soil engineering*. Harper and Row, New York, N.Y.
- Take, W.A. 1998. Lateral earth pressures behind rigid fascia retaining walls. MSE thesis, University of New Brunswick.
- Take, W.A., Valsangkar, A.J. 2001. Earth pressures on unyielding retaining walls of narrow backfill width. *Canadian Geotechnical Journal*, **38**: 1220-1230.
- Terzaghi, K. 1936. Stress distribution in dry and in saturated sand above a yielding trap-door. *Proceedings of 1st International Conference on Soil Mechanics and Foundation Engineering*, Cambridge, Mass., vol. 1, pp. 307-311.
- Terzaghi, K. 1943. *Theoretical Soil Mechanics*. John Wiley & Sons.
- Thomas, E.G., Nantel, J.H., et Notley, K.R. 1979. *Fill Technology in Underground Metalliferous Mines*. International Academic Services, Kingston, Canada.
- Udd, J.E. 1989. Backfill research in Canadian mines. *In* F.P. Hassani, M.J. Scoble, T.R. Yu (eds), *Innovation in Mining Backfill Technology*, pp. 3-13. Rotterdam: Balkema.

- Van Horn, D.A. 1964. A study of loads on underground structures. Proceedings of the Symposium on Soil-Structure Interaction, 8 - 11 June 1964. Tucson, Arizona: University of Arizona, pp. 256-282.
- Williams, J.C., Al-Salman, D., Birks, A.H. 1987. Measurement of static stresses on the wall of a cylindrical container for particulate solids. *Power Technology*, **50**: 163-175.

L'École Polytechnique se spécialise dans la formation d'ingénieurs et la recherche en ingénierie depuis 1873



École Polytechnique de Montréal

**École affiliée à l'Université
de Montréal**

Campus de l'Université de Montréal
C.P. 6079, succ. Centre-ville
Montréal (Québec)
Canada H3C 3A7

www.polymtl.ca

